

1 **Genotype-specific differences in infertile men due to loss-of-function variants in *M1AP***
2 **or *ZZS* genes**

3 Nadja Rotte¹, Jessica E.M. Dunleavy², Michelle D. Runkel¹, Daniela Fietz³, Adrian Pilatz⁴,
4 Johanna Kuss¹, Ann-Kristin Dicke¹, Sofia B. Winge⁷, Sara Di Persio⁵, Christian Ruckert⁶,
5 Verena Nordhoff⁵, Hans-Christian Schuppe⁴, Kristian Almstrup^{7,8}, Sabine Kliesch⁵, Nina
6 Neuhaus⁵, Birgit Stallmeyer¹, Moira K. O'Bryan², Frank Tüttelmann¹, Corinna Friedrich^{1*}

7 ¹Centre of Medical Genetics, Institute of Reproductive Genetics, University of Münster, 48149
8 Münster, Germany

9 ²School of BioSciences and Bio21 Molecular Sciences and Biotechnology Institute, Faculty of
10 Science, University of Melbourne, Parkville, 3010 Australia

11 ³Institute of Veterinary Anatomy, Histology and Embryology, University of Gießen, 35392
12 Gießen, Germany

13 ⁴Clinic and Polyclinic for Urology, Paediatric Urology and Andrology, University Hospital
14 Gießen, 35392 Gießen, Germany

15 ⁵Centre of Reproductive Medicine and Andrology, University of Münster, 48149 Münster,
16 Germany

17 ⁶Department of Medical Genetics, University Hospital Münster, 48149 Münster, Germany

18 ⁷Department of Growth and Reproduction, University Hospital Copenhagen, 2100
19 Copenhagen, Denmark

20 ⁸Department of Cellular and Molecular Medicine, Faculty of Health and Medical Sciences,
21 University of Copenhagen, Denmark

22 ***Correspondence:** Centre of Medical Genetics, Institute of Reproductive Genetics, University
23 of Münster, Vesaliusweg 12-14, 48149 Münster, Germany, corinna.friedrich@ukmuenster.de
of Münster, Vesaliusweg 12-14, 48149 Münster, Germany, and should not be used to guide clinical practice.

M1AP, ZZS & crossover formation

24 **Word count:** 5334 (text), 252 (abstract)

25 **Abstract**

26 Male infertility and meiotic arrest have been linked to *M1AP*, the gene encoding meiosis I
27 associated protein. In mice, M1AP interacts with the ZZS proteins SHOC1, TEX11, and
28 SPO16, which promote DNA class I crossover formation during meiosis. To determine whether
29 M1AP and ZZS proteins are involved in human male infertility by disrupting class I crossover
30 formation, we screened for biallelic or hemizygous loss-of-function (LoF) variants in the
31 encoding human genes to select men with a presumed protein deficiency; we compiled N=10
32 men for *M1AP*, N=4 for *SHOC1*, N=9 for *TEX11*, and the first homozygous LoF variant in
33 *SPO16* in an infertile man. After in-depth characterisation of the testicular phenotype of these
34 men, we identified gene-specific meiotic impairments: men with SHOC1, TEX11, or SPO16
35 deficiency shared an early meiotic arrest lacking haploid germ cells. All men with LoF variants
36 in *M1AP* exhibited a predominant metaphase I arrest with rare haploid round spermatids, and
37 six men even produced sporadic elongated spermatids. These differences were explained by
38 different recombination failures: abrogated SHOC1, TEX11, or SPO16 led to incorrect
39 synapsis of homologous chromosomes and unrepaired DNA double-strand breaks (DSB). On
40 the contrary, abolished M1AP did not affect synapsis and DSB repair but led to a reduced
41 number of class I crossover events. Notably, medically assisted reproduction resulted in the
42 birth of a healthy child, offering the possibility of fatherhood to men with LoF variants in *M1AP*.
43 Our study establishes M1AP as an important, but not essential, functional enhancer in the
44 network of ZZS-mediated meiotic recombination.

45

46 **Keywords: M1AP / meiosis / crossover / infertility / recombination**

47 **Introduction**

48 Worldwide, around one in six adults is infertile (World Health Organization, 2023), and the
49 underlying causes are equally distributed between both sexes (Vander Borgh and Wyns,
50 2018). In men, the most severe forms of infertility are non-obstructive azoospermia (NOA) and
51 cryptozoospermia, meaning that due to spermatogenic failure, no or only few spermatozoa are
52 detected in the ejaculate (Nieschlag et al., 2023). For most of these cases, the only chance of
53 fathering a child is through testicular sperm extraction (TESE) with subsequent medically
54 assisted reproduction (MAR) using intracytoplasmic sperm injection (ICSI).

55 In many of these men, the absence of spermatozoa is caused by an arrest of spermatogenesis
56 at meiosis (termed meiotic arrest or spermatocyte arrest; Wyrwoll et al., 2023b). It has been
57 repeatedly described that this phenotype often arises via monogenic traits (Krausz et al., 2020;
58 Wyrwoll et al., 2023a). One established disease gene for meiotic arrest is *M1AP*, which
59 encodes meiosis 1 associated protein (Wyrwoll et al., 2020). In mice, M1AP has recently been
60 shown to interact with three well-characterised meiosis-related proteins: SHOC1, TEX11, and
61 SPO16 (Li et al., 2023). These form a highly conserved complex, called ZZS (from yeast
62 Zip2/Zip4/Spo16), that in many species is crucial during prophase I of meiosis (De Muyt et al.,
63 2018). However, it remains unknown whether the same applies for human ZZS and M1AP.

64 Meiosis is the crucial process during spermatogenesis that leads to the formation of haploid
65 germ cells. A key step during meiosis is homologous recombination, which is required for
66 accurate chromosome segregation and the formation of haploid gametes. Homologous
67 recombination, which also enables genetic diversity, occurs via crossovers between
68 homologous chromosomes (chiasmata). Briefly, the process is initiated by programmed DNA
69 double-strand breaks (DSB) in early prophase I (Figure 1A). At the end of this phase, the DSBs
70 are repaired and resolved as either non-crossovers or crossovers. When at least one
71 crossover per homologous chromosome is formed, correct segregation can ensue; this is the
72 *obligatory crossover* principle (repeatedly reviewed in (Bolcun-Filas and Handel, 2018; De
73 Massy, 2013; Gray and Cohen, 2016; Xie et al., 2022)).

M1AP, ZZS & crossover formation

74 In humans, there are approximately 50 crossovers per spermatocyte, which translates to one
75 to five crossovers per pair of homologous chromosomes (Sun et al., 2005). During meiosis,
76 meiotic recombination is mediated by a subset of highly conserved proteins of the ZMM family
77 (an acronym for the yeast proteins Zip1/Zip2/Zip3/Zip4, Msh4/Msh5, Mer3, and Spo16;
78 reviewed in Pyatnitskaya et al., 2019), including ZZS proteins. In particular, these proteins
79 assemble within a meiosis-specific structure, the synaptonemal complex (SC), support the
80 synapsis of homologous chromosomes and stabilise recombination intermediates (reviewed
81 in Zickler and Kleckner, 2015). Only when the intermediates are stabilised by ZMM, the DSBs
82 can be resolved as class I crossovers (Börner et al., 2004).

83 Even minor errors in this tightly coordinated interplay can lead to meiotic arrest and infertility
84 (Xie et al., 2022). Accordingly, genetic variants in each of the ZZS genes have already been
85 linked to meiotic arrest in humans, with the typical phenotypes being NOA in men and
86 primary/premature ovarian insufficiency (POI) in women. The ZZS gene *TEX11* is a well-
87 established X-linked gene for clinical diagnostics in male infertility (Wyrwoll et al., 2023a;
88 Yatsenko et al., 2015); biallelic pathogenic variants in *SHOC1* lead to infertility in men and
89 women (Krausz et al., 2020; Ke et al., 2023); and one homozygous splice region variant in
90 *SPO16* has recently been associated with POI (Qi et al., 2023). While a strong association
91 between *M1AP* and male infertility has been demonstrated (Wyrwoll et al., 2020; Li et al.,
92 2023), the protein's molecular function remains unexplored in humans.

93 In this study, we identified that human M1AP interacts *in vitro* with each of the ZZS proteins.
94 Additionally, we present the first man homozygous for a loss-of-function (LoF) variant in
95 *SPO16*. The testicular phenotype of this man and men with LoF variants in the other ZZS
96 genes *SHOC1* and *TEX11* shared an early prophase I arrest including asynapsis and
97 unrepaired DSBs. In contrast, LoF variants in *M1AP* led to a metaphase I arrest, where early
98 meiotic recombination was completed while the total number of the final recombination
99 products, the meiotic class I crossover events, was reduced. Ultimately, this leads to a
100 predominant meiotic arrest, but fertilisation-competent spermatozoa have on rare occasions

M1AP, ZZS & crossover formation

101 been retrieved by testicular sperm extraction. This demonstrates that M1AP is an important
102 but not essential functional enhancer in the complex network of meiotic recombination.
103 Collectively, these genotype-specific differences have important clinical implications, as they
104 can be used to guide evidence-based treatment decisions or counselling of couples with male-
105 factor infertility.

106

107 **Results**

108 **Human M1AP interacts with the ZZS proteins SHOC1, TEX11, and SPO16 *in vitro* and**
109 **shares a similar mRNA expression profile**

110 To assess interaction between the ZZS proteins and M1AP in humans, we performed co-
111 immunoprecipitation (IP). Human DYK-tagged M1AP was co-expressed with human HA-
112 tagged SHOC1, TEX11, or SPO16 in HEK293T cells. Proteins were immunoprecipitated from
113 cell lysates by tag-specific antibodies. A subsequent Western blot showed that human M1AP
114 binds specifically to each of the three ZZS complex components (Figure 1B), showing that
115 M1AP interacts with the ZZS complex in humans. Assuming a closely related function of all
116 four proteins in human meiosis, we aimed to investigate whether all four genes share a similar
117 testicular expression profile. Thus, previously published single-cell RNA sequencing data of
118 human testicular tissue (Di Persio et al., 2021) were queried (Figure 1C). Overall, the analysis
119 showed that all four genes are similarly expressed in all stages of meiosis with strong mRNA
120 abundance during early prophase I (leptotene, zygotene). *SHOC1* and *TEX11* showed an
121 additional increase of expression during later meiotic divisions.

122 **Composition of the study cohort with men carrying LoF variants in *M1AP* or ZZS**

123 To compare the protein-related impact of each of the four proteins on human meiosis, we
124 selected cases carrying LoF variants in either *M1AP* (NM_138804.4) or one of the ZZS
125 components encoding genes, *SHOC1* (NM_173521.5), *TEX11* (NM_001003811.2), and
126 *SPO16* (NM_001012425.2) from our Male Reproductive Genomics (MERGE) study cohort. In
127 addition, we included one published case with a variant in *SHOC1* from the GEMINI cohort
128 (Nagirnaja et al., 2022; G-377). Both previously published (N=10) and novel (N=14) cases
129 were considered for functional in-depth analysis.

130 We compared the phenotypes of ten unrelated men with homozygous LoF variants in *M1AP*,
131 four with biallelic LoF variants in *SHOC1*, nine with hemizygous LoF variants in *TEX11*, and
132 one man with a homozygous LoF variant in *SPO16* (Figure 1D, Table 1). Nine of the men with
133 a LoF variant in *M1AP* carried the recurrent pathogenic frameshift variant c.676dup, of which

M1AP, ZZS & crossover formation

134 four had already been published and functionally analysed (Wyrwoll et al., 2020) while one
135 man (M3609) carried a homozygous *M1AP* splice site variant (c.1073_1074+10del). This
136 variant was predicted to undergo nonsense-mediated decay. The functional significance was
137 analysed *in vitro* by a minigene assay which demonstrated aberrant splicing (Appendix
138 Figure S1).

139 For *SHOC1*, we selected two men (M2012, G-377) carrying the same homozygous frameshift
140 variant (c.1085_1086del) and one case (M2046) with confirmed compound heterozygous
141 variants (c.[1351del;1347T>A];[945_948del]), who were previously described (Table 1; Krausz
142 et al., 2020; Nagirnaja et al., 2022). In addition, a novel splice site variant (c.1939+2T>C) was
143 identified in one man (M3260). The *in vitro* minigene assay showed aberrant splicing resulting
144 in an in-frame exon skipping event involving only ~4% of the total protein (Appendix Figure S2)
145 and may not lead to a complete loss of but only to a reduced protein function. This deletion
146 affects the distant helicase hits region but not the highly conserved ‘SHOC1 homology region’,
147 which is important for the interaction with the other ZZS proteins (Macaisne et al., 2008).

148 The cohort of nine men with hemizygous LoF variants in *TEX11* comprised three men with
149 different partial gene deletions, of which two were inherited from the mother (Appendix Figures
150 S17/S18), two men with splice site variants, and four men with variants encoding premature
151 stop codons (Table 1); three of these cases have already been described but not in this detail
152 (Wyrwoll et al., 2023a; Yatsenko et al., 2015).

153 One man (M3863) carried a novel homozygous frameshift variant (c.266del p.(Leu89Trpfs*15))
154 in the highly conserved ZZS gene *SPO16* (Table 1). This variant was predicted to induce a
155 premature stop codon in exon 4 and to truncate >40% of the complete protein. Most of the
156 protein's central domain and the entire functional helix-hairpin-helix (HhH) domain would be
157 affected by the truncation (Appendix Figure S3). According to the prediction, it was more likely
158 that the mRNA was degraded by nonsense-mediated decay. In both cases, a loss of protein
159 function can be expected.

M1AP, ZZS & crossover formation

160 Semen analysis of all 24 men included in this study revealed a high proportion of azoospermia
161 (N=21), with the remaining three men displaying cryptozoospermia. Interestingly, all three
162 cryptozoospermic men were homozygous for the recurrent LoF variant in *M1AP* (c.676dup).
163 Clinical features were similar between men, including normal testicular volumes, normal
164 luteinising hormone, follicle-stimulating hormone in the high range, and normal testosterone
165 (Appendix Table S1; Appendix Figure S4).

166 **Men with LoF variants in *M1AP* or *ZZS* showed gene-specific spermatogenic defects**

167 Testicular biopsies originating from testicular sperm retrieval (TESE) procedures were
168 available in 21 of the selected cases and used for histological evaluation of spermatogenic
169 differentiation. Analysis using periodic acid-Schiff (PAS, N=14) or haematoxylin and eosin
170 (H&E, N=6) staining determined a common testicular phenotype of predominant spermatocyte
171 arrest in all cases (Human Phenotype Ontology [HPO] term: HP:0031039, Figure 2A;
172 Appendix Figure S5/S6). In addition, we observed cells in diakinesis or metaphase I stage
173 characterised by scattered and misaligned chromosomes (Figure 2A, detail view). Of note, we
174 only saw metaphase cells with correctly aligned chromosomes in controls and in men with LoF
175 variants in *M1AP*.

176 To analyse the presence of post-meiotic germ cells, we performed immunohistochemical
177 staining for cAMP responsive element modulator (CREM), a marker protein for round
178 spermatids (Weinbauer et al., 1998). Tissue of 16 men was available for subsequent analysis
179 (Figure 2B, Appendix Figure S7). In fertile control samples (N=3), CREM positive spermatids
180 were observed in almost all tubules with an average 30.42 ± 1.20 spermatids per tubule. In all
181 men analysed with LoF variants in *M1AP* (N=7), CREM-positive spermatids were observed
182 however in significantly lower numbers than controls with an average of 0.50 ± 0.16 cell/tubule.
183 Indeed, some but not all seminiferous tubules were found to contain round spermatids, and
184 elongated spermatids were only observed in six of these cases. In contrast, CREM-positive
185 round spermatids were only observed in one man with a splice site variant in *SHOC1* (M3260),
186 which presumably not causes a loss of protein function but only an impairment of SHOC1

187 function enabling significantly reduced progression of spermatogenesis up to the round
188 spermatid stage in occasional cells (Appendix Figure S2E). In total, we detected much fewer
189 of this germ cell subtype in M3260 than in cases with LoF variants in *M1AP*. In addition, we
190 detected no CREM-positive round spermatids in cases with LoF variants in *SHOC1* or *TEX11*.
191 The single case with a homozygous LoF in *SPO16* (M3863) exhibited complete meiotic arrest
192 without CREM-positive round spermatids. These results demonstrate a different testicular
193 phenotype between men with LoF variants in *M1AP* and men affected by LoF variants in key
194 components of the ZZS complex (Figure 2C).

195 **Proper chromosome synapsis and XY body formation despite M1AP deficiency**

196 To assess whether the LoF variants in *M1AP* and in ZZS genes led to the impaired production
197 of post-meiotic cells because of alterations in meiotic recombination, we stained patients'
198 testicular tissue for the two key meiosis markers γ H2AX and H3S10p. Phosphorylated histone
199 variant H2AX (γ H2AX) is a marker for DSBs and was used to analyse DSB repair and correct
200 synapsis of homologous chromosomes. In autosomes, DSBs are repaired once the
201 homologues have successfully aligned and synapsed, and, consequently, γ H2AX staining
202 disappears. In parallel, when meiotic sex chromosome inactivation (MSCI) takes place during
203 pachytene, a condensed chromatin domain is formed, termed the XY body. Here, γ H2AX
204 accumulates independent of meiotic recombination-associated DSBs (Fernandez-Capetillo et
205 al., 2003). Together, the DSB repair in autosomes and the distinct formation of the XY body
206 suggest that cells are passing through the pachytene checkpoint (Hamer et al., 2003).

207 Figure 3A shows the distinct γ H2AX localisation during meiosis I prophase and metaphase in
208 a human control. Men with LoF variants in *M1AP* were characterised by a qualitatively
209 equivalent staining pattern, with quantitatively reduced amounts of pachytene- and increased
210 amounts of zygotene-like cells (Figure 3A, detail view, bar graph, Appendix Figure S8).
211 Interestingly, the complete repair of DSBs post-zygotene-like and the clear restriction of γ H2AX
212 to the XY body was only observed in controls and in men with LoF variants in *M1AP*. In men
213 with LoF variants in *SHOC1*, *TEX11*, or *SPO16*, most of the cells maintained a zygotene-to-

M1AP, ZZS & crossover formation

214 pachytene-like stage with enlarged nuclei, accumulated DSBs, and aberrant γ H2AX
215 localisation (Figure 3A, detail view, bar graph, Appendix Figure S9). Thus, an arrest in these
216 men occurs between zygotene- to early pachytene-like (Z^*/P^*), referring to a human type I
217 meiotic (Jan et al., 2018) or pachytene arrest (Enguita-Marruedo et al., 2019). Remarkably,
218 even though cells do not proceed properly beyond zygotene-pachytene-like stage in the
219 majority of men with LoF variants in *SHOC1*, *TEX11*, or *SPO16*, γ H2AX-positive metaphase-
220 like or diakinesis cells (M-I*) were seen in most of the cases (N=8). These cells were
221 characterised by their spatial distribution within the tubules and scattered chromosomes,
222 incorrectly aligned at the metaphase plate or maintained in a diakinesis stage. While similar
223 cells were seen in men with LoF variants in *M1AP*, we also observed in parallel γ H2AX-
224 negative, intact metaphase cells with properly aligned chromosomes (N=7).

225 In addition, we used phosphorylated histone 3 (H3S10p) to mark cells reaching the metaphase
226 stage (Song et al., 2011). H3 is phosphorylated when the DNA is condensed during mitosis
227 and meiosis for subsequent segregation of the chromosomes. Localisation of H3S10p in all
228 cases with LoF variants in *M1AP* showed that the cells with properly aligned chromosomes
229 are meiotic metaphase cells (Appendix Figure S10). This, together with the presence of post-
230 meiotic cells, classified the arrest in men with *M1AP* LoF variants as a partial metaphase I
231 arrest (Enguita-Marruedo et al., 2019). In accordance with the γ H2AX staining, localisation of
232 H3S10p in men with LoF variants in *SHOC1*, *TEX11*, or *SPO16* revealed only aberrant
233 metaphase-like/diakinesis-stage (M-I*) or mitotic spermatogonia (Appendix Figure S10).

234 **Increased apoptosis leads to a loss of germ cells**

235 Maintenance of γ H2AX localisation in metaphase I cells indicates a failure of meiotic
236 recombination and checkpoint-induced apoptotic events (Enguita-Marruedo et al., 2019).
237 Thus, we quantified apoptotic DNA fragmentation via TUNEL assay. Compared to controls, we
238 observed a significant increase in apoptosis for all patients analysed (Figure 3B,
239 Appendix Figure S11). Most TUNEL-positive cells showed hallmarks of apoptosis, namely
240 condensation, fragmentation, and apoptotic bodies (Saraste and Pulkki, 2000). In addition,

241 aberrant metaphase I-like cells with misaligned chromosomes or diakinesis-like stage cells (M-
242 I*) were also TUNEL-positive (Figure 3B, detail view). In cases with LoF variants in *SHOC1*,
243 *TEX11*, and *SPO16*, apoptotic DNA fragmentation was also found in rare pre-metaphase
244 spermatocytes. One key difference between the cases was that only men with LoF variants in
245 *M1AP* exhibited TUNEL-negative metaphase cells, round, and even elongated spermatids.

246 **Sufficient class I crossover events occurred despite *M1AP* LoF variants**

247 To address whether meiotic recombination was successfully completed in spermatocytes from
248 men with LoF variants in *M1AP*, allowing them to differentiate into post-meiotic haploid cells,
249 we analysed spermatocyte spreads of one man (M864). In comparison, we determined the
250 recombination failure in one man each with a LoF variant in *SHOC1* (M2046), *TEX11* (M3409),
251 or *SPO16* (M3863). To indicate whether the synaptonemal complex (SC) formed properly, we
252 stained for SYCP1 and SYCP3-containing elements of the SC that assemble along unaligned
253 chromosome axes (Yuan et al., 2000). For crossover formation to occur, homologous
254 chromosomes must undergo full synapsis, which is fulfilled when the transverse filament
255 protein of the SC, SYCP1, localises between the axes (Dunce et al., 2018). To visualise
256 designated crossover sites, we stained for MLH1, an endonuclease involved in the resolution
257 of class I crossovers (Baker et al., 1996). To quantify class I crossover, we counted MLH1 foci
258 in pachytene cells (n=10). In addition, to determine the progression of prophase I, we stained
259 for γ H2AX. Further, to analyse the correct recruitment of the ZZS complex, we labelled *TEX11*.
260 For a better orientation, we marked the centromeres using a human anti-centromere antibody
261 (ACA) (Figure 4A/B cyan, Appendix Figure S12/S13 cyan).

262 Similar to the control, we observed spermatocytes of M864 (LoF variant in *M1AP*) in the
263 pachytene-like stage, including properly formed chromosome axes (SYCP3) and fully
264 synapsed homologues (SYCP1). In addition, class I crossovers were indicated by MLH1 foci
265 (Figure 4A). In contrast, in men with *SHOC1*, *TEX11*, or *SPO16* deficiency, no pachytene-like
266 spermatocytes were identified (Figure 4B, Appendix Figure S12/S13). In all three cases,
267 accumulated γ H2AX domains were observed (Appendix Figure S13 red). In addition, SYCP1

268 assembly was highly reduced in M2046 (SHOC1) and facilitated to some extent in M3409
269 (TEX11) and M3863 (SPO16; Figure 4B red, Appendix Figure S12 red). Moreover, TEX11 was
270 completely absent in M3409 (TEX11) and highly reduced and disorganised in M2046 (SHOC1)
271 and M3863 (SPO16; Appendix Figure S13 magenta). In contrast, in M864 (M1AP),
272 spermatocytes reached the pachytene-like stage, had resolved DSBs (γ H2AX), and showed
273 reduced but successful TEX11 recruitment to the chromosome axes (Appendix Figure S13
274 red). Importantly though, the man with a LoF variant in *M1AP* showed fewer designated
275 crossover sites per spermatocyte (via quantification of MLH1 foci) than the control (Figure 4B
276 magenta). Specifically, the man had on average 34.5 ± 2 MLH1 foci per spermatocyte vs. 48 ± 2
277 foci per control spermatocyte.

278 One crucial principle of meiotic recombination is the acquired number of crossovers per pair
279 of homologous chromosomes, called the *obligatory crossover*. This means that each pair forms
280 at least one crossover, crucial for the subsequent equilibrated segregation during meiosis I
281 (reviewed in Wang et al., 2015). Taking advantage of super resolution structured illumination
282 microscopy (SR-SIM), we investigated whether this principle was still fulfilled when M1AP was
283 presumably dysfunctional (Figure 4C). MLH1 foci (dotted circles) were marked on each pair of
284 homologous chromosomes from one representative spermatocyte of the man with a LoF
285 variant in *M1AP* to localise the sites of class I crossovers. In total, 36 MLH1 foci were seen in
286 this example, and all paired chromosomes showed at least one MLH1 focus, ensuring the
287 obligatory crossover principle in this set of designated chromosomes.

288 **Men with LoF variants in *M1AP* can father healthy children by MAR**

289 Four of the ten men with LoF variants in *M1AP* tried to conceive via ICSI. Two men (M2062
290 and 2746) were counselled about their genetic diagnosis before trying MAR. So far, only one
291 man, M2746, has successfully fathered a healthy child following ICSI with ejaculated sperm.
292 In the first and second ICSI attempts, oocyte fertilisation was possible, but cells did not develop
293 to the blastocyst stage or did not lead to a clinical pregnancy. In the third attempt, nine oocytes
294 were fertilised, seven of which developed up to the two-pronuclei (2N) stage. Two reached the

M1AP, ZZS & crossover formation

295 blastocyst stage and were transferred to the female partner, after which one successfully
296 implanted and developed normally, resulting in the birth of a healthy boy. Genome sequencing
297 data of the child's genomic DNA compared to the father's demonstrated the paternity and the
298 inheritance of the *M1AP* frameshift variant in a heterozygous state (Figure 5A). In an ICSI-
299 TESE attempt by M2062 and his female partner, three oocytes were fertilised, but none
300 developed to the blastocyst stage and a transfer was not possible. For M3402 and his female
301 partner, two ICSI attempts were not successful. For M3511, five spermatozoa were retrieved
302 by TESE and used for ICSI; however, none of the five injected oocytes were fertilised.

303 To rule out any aneuploidies in the newborn boy, genome sequencing coverage data were
304 analysed, and aberrations were excluded (Appendix Figure S14). Considering the exemplary
305 case of M2746, ICSI with ejaculated spermatozoa or spermatozoa recovered from TESE offers
306 the possibility of fatherhood for men with LoF variants in *M1AP* (Figure 5B).

307

308 **Discussion and conclusion**

309 Indications that *M1AP* is required for mammalian spermatogenesis date back to 2006, when
310 the mouse orthologue was demonstrated to be expressed in male germ cells during the late
311 stages of spermatogenesis (Arango et al., 2006). This was strengthened by two subfertile
312 mouse models with predominant meiotic arrest, hinting toward the protein's role during male
313 meiosis (Arango et al., 2013; Li et al., 2023). In addition, several human cases of male infertility
314 have been described in which azoo-, crypto-, or extreme oligozoospermia have been
315 associated with biallelic variants in *M1AP* (Wyrwoll et al., 2020; Tu et al., 2020; Li et al., 2023;
316 Khan et al., 2023). Accordingly, *M1AP* has achieved a strong clinical gene-disease association
317 based on the criteria of the Clinical Genome Resource (ClinGen) Gene Curation Working
318 Group, and, therefore, we have proposed that this gene be included in routine diagnostics of
319 infertile men (Wyrwoll et al., 2023a). Recently, *M1AP* was proposed as a fourth component of
320 the mouse ZZS complex, linking its role to three well-known and highly conserved meiosis-
321 related proteins: SHOC1, TEX11, and SPO16 (Li et al., 2023). In our study, we analysed the
322 interaction between *M1AP* and the human ZZS proteins and showed that each ZZS protein
323 bound to *M1AP* independently.

324 The men with LoF variants in *M1AP* investigated in this study displayed a predominant meiotic
325 arrest with occasional haploid germ cells. Our in-depth characterisation of the patients'
326 testicular phenotype implied a partial metaphase I arrest, which was also seen in another
327 reported man with a *M1AP* LoF variant (Li et al., 2023). In addition, we observed the activation
328 of the spindle-assembly checkpoint, which is crucial for preventing premature chromosome
329 separation and, thus, abnormal segregation and aneuploidies (reviewed in Lane and Kauppi,
330 2019). Accordingly, meiotic recombination was presumably intact in individual cells that
331 progressed beyond this checkpoint. As such, an individual fertilisation-competent
332 spermatozoon was allowed to develop, ultimately resulting in the birth of a healthy, euploid
333 child.

M1AP, ZZS & crossover formation

334 These findings in humans mimic the *M1ap* knockout mouse model, which was also
335 characterised by male subfertility (Li et al., 2023) with lower sperm counts and an increased
336 number of arrested metaphase I cells with unaligned chromosomes. Here, fewer
337 recombination intermediates and reduced crossover events led to metaphase I arrest and
338 cellular apoptosis, and, consistent with the human variant carriers' phenotype, only a fraction
339 of cells progressed to fertility-competent spermatozoa.

340 In humans, *SHOC1* and *TEX11*, which encode two of the M1AP binding partners in the meiotic
341 ZZS complex, have also previously been associated with male infertility and meiotic arrest
342 (Krausz et al., 2020; Yatsenko et al., 2015), and both genes represent validated disease genes
343 for male infertility (Wyrwoll et al., 2023a). In contrast to *M1AP*, hemizygous and biallelic LoF
344 variants in these genes, respectively, have primarily been associated with a complete lack of
345 haploid germ cells (Yatsenko et al., 2015; Krausz et al., 2020). However, the evaluation of the
346 testicular phenotype in these initial reports was based on testicular overview staining, making
347 a definitive conclusion difficult. In this study, we concordantly observed complete meiotic arrest
348 and a lack of haploid, CREM-positive germ cells in all men we analysed with LoF variants in
349 *TEX11*, pointing to an activation of the first, the pachytene, checkpoint (Yatsenko et al., 2015;
350 Yu et al., 2021) and to an invariable genotype-phenotype correlation. This congruent
351 phenotype was also observed in two men with LoF variants in *SHOC1*. Only in one patient with
352 a homozygous splice site variant in *SHOC1* did we detect CREM-positive round spermatids.
353 This splice site variant induces the in-frame deletion of a single exon. The resulting protein
354 may still have reduced function and maintained interaction to the other ZZS proteins, due to a
355 preserved XPF-ERCC1-like complex formation and a partly maintained distant helicase hits
356 region, as described similarly for yeast and mouse mutants (De Muyt et al., 2018; Guiraldelli
357 et al., 2018).

358 In contrast to *TEX11* and *SHOC1*, biallelic variants in *SPO16* have so far only been linked to
359 female infertility (Qi et al., 2023); thus, our study demonstrates the first case of an infertile man
360 with a biallelic LoF variant in *SPO16*, highlighting it as a novel candidate gene also for male

M1AP, ZZS & crossover formation

361 infertility. His testicular phenotype and type of spermatogenic arrest is comparable to that of
362 *TEX11* and *SHOC1* variant carriers, where no haploid germ cells were detected. Again, DSBs
363 remain persistent and complete synapsis of chromosomes were lacking. In line, crossover
364 resolution was absent, resulting in a complete meiotic arrest. In conclusion, in-depth testicular
365 characterisation of the large number of men with LoF variants in *TEX11* points to a genotype-
366 specific phenotype that correlates with the phenotype of the other two key ZZS genes, *SHOC1*
367 and *SPO16*. However, further identification of cases is needed to fully understand how the loss
368 of SHOC1 and SPO16 function affects meiotic progression.

369 Our observations on human cases are substantiated by described mouse models targeting the
370 orthologues of the respective genes, which displayed sterility and an early spermatocyte arrest
371 (Yang et al., 2008; Zhang et al., 2019, 2018). *Tex11* knockout mice were associated with male
372 sterility due to apoptosis of spermatocytes, asynapsis of homologues, delayed DSB repair, and
373 a decreased number of crossover events (Yang et al., 2008). Both complete and germ cell-
374 specific knockout of *Shoc1* resulted in sterility. Germ cell arrest varied between zygotene and
375 mid-pachytene stages, and cells lacked distinct XY bodies, complete chromosomal synapsis,
376 and crossover events (Zhang et al., 2018). Homozygous knockout of *Spo16* in mice led to
377 sterility, impaired chromosome pairing, and reduced crossover formation (Zhang et al., 2019).
378 Compared to *Shoc1*, the *Spo16* knockout mice displayed milder defects in DSB repair and
379 synapsis, indicating that SHOC1 alone maintains partially functionality and enables reduced
380 DSB repair.

381 The common basis of all four genes *M1AP*, *SHOC1*, *TEX11*, and *SPO16*, is male infertility and
382 meiotic arrest in the case of a loss of protein function. However, this study identified striking
383 differences in the testicular phenotype of men with LoF variants in *M1AP* in contrast to those
384 patients affected by LoF variants in the main ZZS complex genes *SHOC1*, *TEX11*, and *SPO16*.
385 To explain why M1AP deficiency still allows a fraction of germ cells in men and mice to progress
386 through meiosis to the haploid germ cell stage, we argue that even in the absence of M1AP, a
387 reduced SHOC1-TEX11-SPO16 interplay is maintained: SHOC1 forms a heterodimer with

M1AP, ZZS & crossover formation

388 SPO16 that recognises DNA-joined molecules and binds to and stabilises early recombination
389 intermediates (Guiraldelli et al., 2018; Zhang et al., 2019). TEX11 is recruited to these sites
390 and, in turn, assists in recruiting meiosis-specific proteins such as SYCP2 and MutSy (MSH4-
391 MSH5), which are needed to facilitate synaptonemal complex assembly and DSB repair, finally
392 yielding to crossover formation (Yang et al., 2008; Zhang et al., 2018).

393 Our findings indicate that M1AP is an important functional enhancer for promoting meiotic
394 resolution in the ZZS network, but it is not mandatory. This is supported by the fact that
395 although meiosis is an evolutionarily highly conserved process (reviewed in Börner et al.,
396 2023), and, accordingly, the ZZS proteins Zip2 (SHOC1), Zip4 (TEX11), and Spo16 (SPO16)
397 play an essential role in meiotic recombination in yeast, this lower eukaryote has no M1AP
398 orthologue. While yeast is a well-established model organism for meiosis, M1AP is only
399 conserved down to fish species, indicating that this protein's function in meiotic progression is
400 evolutionarily younger than those of the ZZS complex.

401 In contrast to male meiosis in mice and humans, where deficiency in M1AP or ZZS complex
402 components results in subfertility or infertility, the role of these proteins in female fertility is less
403 clear. In mice, female *M1ap* and *Tex11* knockouts are fertile, albeit with a reduced litter size in
404 the case of *Tex11* knockout (Arango et al., 2013; Li et al., 2023; Yang et al., 2008). Murine
405 *Shoc1* and *Spo16* knockouts display sterility in both sexes (Zhang et al., 2019, 2018), and in
406 humans, biallelic LoF variants in *SHOC1* and *SPO16* have been described to lead to female
407 infertility. For *TEX11*, only women with heterozygous variants have been found to retain their
408 fertility (Wyrwoll et al., 2023a). For *M1AP*, however, because we and others have not identified
409 biallelic variants in *M1AP* in fertile or infertile women, we cannot yet define the role of M1AP in
410 human female meiosis.

411 *M1AP* is a clinically relevant gene for male fertility. The TESE success rate in our cohort was
412 40%, and we described one man who fathered a healthy, euploid child, thus showing that
413 biallelic LoF variants in *M1AP* are compatible with fatherhood and, thereby, presenting a proof-
414 of-principle. However, further studies are needed to fully elucidate the underlying molecular

M1AP, ZZS & crossover formation

415 mechanisms and enable a risk estimation of checkpoint failure and aneuploidy in these men.
416 Accordingly, it currently remains elusive whether all altered cells in men with LoF variants in
417 *M1AP* indeed undergo checkpoint-induced apoptosis or whether rare exceptions develop
418 independently of the spindle-assembly checkpoint resulting in aneuploid spermatozoa.

419 The majority of aneuploid embryos are not viable, frequently leading to spontaneous abortion
420 (Hassold and Hunt, 2001). While studies have suggested an equal fertilisation capability
421 between aneuploid and euploid spermatozoa, they have also evidenced a correlation between
422 high sperm aneuploidy and recurrent ICSI or MAR failure as well as lower rates of pregnancy
423 and live birth (reviewed in Ioannou et al., 2019). ICSI attempts with spermatozoa from two men
424 with LoF variants in *M1AP* (M2062 and M2746) succeeded in fertilising the oocytes. Most of
425 these did, however, not develop to the blastocyst stage or did not lead to a clinical pregnancy.
426 Aneuploid spermatozoa could be one potential explanation for this, especially concerning
427 chromosomes 21, 22, X, and Y, as these typically have a single recombination event and are,
428 thus, more prone to progress without the obligatory crossover (Ferguson et al., 2007; Sun et
429 al., 2008). This hypothesis could not be substantiated by our data, because we could not
430 perform a direct analysis of the very few spermatozoa from any of the men to assess the
431 frequency of aneuploidies. Thus, subsequent studies are needed to answer this question. So
432 far, couples with M1AP-related male-factor infertility should be counselled about the small but
433 existed chance to conceive a chromosomally-balanced biological child but also about the
434 potential risks of aneuploidies and could benefit from preimplantation genetic testing for
435 aneuploidy (PGT-A). Whereas the benefits of PGT-A in unexplained recurrent pregnancy
436 failure cases remain uncertain, some studies focussing on male-factor infertility have shown
437 improved clinical MAR outcomes after PGT-A (Rodrigo et al., 2019; Xu et al., 2021) – and
438 M1AP-associated infertility may be such a case.

439 Both *M1AP* and *TEX11* represent two of the most frequently identified monogenic causes for
440 NOA in men (Yang et al., 2015; Nagirnaja et al., 2022; Wyrwoll et al., 2023b). By identifying
441 the first man with an underlying LoF variant in *SPO16*, we expand the clinical relevance of

M1AP, ZZS & crossover formation

442 genetic causes to all three main ZZS genes and underline their overall importance. Here, we
443 present the first detailed description of the testicular phenotypes of affected men, which is
444 important for inferring the function of the proteins involved. At least for *M1AP* and *TEX11*, we
445 provide for the first time a clear genotype-phenotype correlation, as men with LoF in the same
446 gene show a concordant phenotype. As a result, it will now be possible to distinguish likely
447 pathogenic variants in *TEX11* and *M1AP* from likely benign variants, i.e., those less likely to
448 have a functional effect. Specifically, pathogenic missense variants in these genes leading to
449 abolished protein function are expected to lead to the described, highly specific testicular
450 phenotype. To the best of our knowledge, our study is also the first report on the birth of a
451 healthy child (reviewed in Xie et al., 2022) having a father with a pathogenic gene variant in a
452 clinically established disease gene for NOA. This not only distinguishes *M1AP* from other NOA
453 genes, but it also shows that human M1AP, in contrast to the other ZZS proteins, is not required
454 for class I crossover formation. Future studies should further address the functional links and
455 underlying molecular details between M1AP and the human ZMM machinery.

456 **Material/subjects and methods**

457 **Study cohort**

458 The Male Reproductive Genomics (MERGE) study comprised exome (N=2,629) and genome
459 sequencing (N=74) datasets of overall 2,703 probands (for details see Appendix Methods). It
460 includes men with various infertility phenotypes: 1,622 men with azoospermia (no spermatozoa
461 in the ejaculate, HP:0000027), 487 men with cryptozoospermia (spermatozoa only identified
462 after centrifugation, HP:0030974), 380 men with varying oligozoospermia (total sperm count:
463 >0 to <39 million spermatozoa, HP:0000798), 188 men with a total sperm count above 39
464 million, and 26 family members. Established causes for male infertility including previous radio-
465 or chemotherapy, hypogonadotropic hypogonadism, Klinefelter syndrome, or microdeletions
466 of the azoospermia factor (AZF) regions on the Y-chromosome were exclusion criteria. All men
467 underwent routine physical and hormonal analysis of luteinising hormone (LH), follicle-
468 stimulating hormone (FSH), testosterone (T) as well as semen analysis according to the
469 respective WHO guidelines.

470 For this study, we selected men with rare biallelic (minor allele frequency [MAF] in gnomAD
471 database v2.1.1, ≤ 0.01) or hemizygous (MAF ≤ 0.001) loss-of-function (LoF) variants (stop-,
472 frameshift-, splice site variants) and deletions in *M1AP*, *SHOC1* [*C9orf84*], *TEX11*, and
473 *C1orf146* [*SPO16*]. For consistency in the manuscript, we used the HGNC
474 (<https://www.genenames.org/>) approved gene symbols for *M1AP*, *SHOC1*, and *TEX11*,
475 whereas we refer to *C1orf146* using its alias gene symbol, *SPO16*. As a reference, the longest
476 transcript with the highest testicular expression was chosen (*M1AP*: NM_001321739.2,
477 *SHOC1*: NM_173521.5, *TEX11*: NM_1003811.2, *SPO16*: NM_001012425.2). If possible,
478 segregation analysis was conducted on the DNA of family members. Samples with qualitatively
479 and quantitatively normal spermatogenesis were included as controls (M2132, M2211, M3254,
480 Appendix Figure S15, statistical analyses). In addition, one previously published case from an
481 external cohort (GEMINI-377, referred to as G-377) was included for subsequent analysis
482 (Nagirnaja et al., 2022).

483 **Ethical approval**

484 All individuals gave written informed consent compliant with local requirements. The MERGE
485 study was approved by the Ethics Committee of the Ärztekammer Westfalen-Lippe and the
486 Medical Faculty Münster (Münster #2010-578-f-S, #2012-555-f-S; Giessen #26/11); the study
487 of GEMINI-377 was approved by the ethics committee for the Capital Region in Denmark (#H-
488 2-2014-103), all in accordance with the Helsinki Declaration of 1975.

489 **Cell culture and transient (co-)transfection experiments**

490 Human embryonic kidney (HEK) 293T cells were cultured in Dulbecco's modified Eagle
491 medium (DMEM) with 10% foetal calf serum (FCS) and 1% penicillin/streptomycin (PS). The
492 culture was maintained in T75 cell culture flasks at 37°C, 5% CO₂, and 85% humidity.

493 For overexpression experiments, 400,000 cells per well were seeded in 6-well plates,
494 cultivated for two days in DMEM-FCS without PS, and transfected at 80-100% confluence
495 using the K2® transfection system (Biontexas, #T060) according to the manufacturer's
496 instructions. Briefly, K2® maximiser reagent was added two hours before transfection. Directly
497 before transfection, the medium was supplemented with 100 µm chloroquine diphosphate salt
498 (Sigma-Aldrich, #C6628). Subsequently, 4 µg cDNA, 260 µl Opti-MEM™ reduced serum
499 medium (Gibco, #31985062), and 9 µl K2® transfection reagent per well were mixed,
500 incubated for 15 minutes, and added to the cells. For co-transfection of DYK-tagged *M1AP*
501 (NM_001321739.2) and either HA-tagged *SHOC1* (NM_173521.5), *TEX11* (NM_031276.3), or
502 *SPO16* (NM_001012425.2), the total amount of DNA was maintained, and the cDNA ratio was
503 adapted according to the respective size of each gene. Transfection and subsequent analysis
504 were performed in three independent replicates minimum and three wells were pooled per
505 replicate.

506 Cell lysis was performed 24 hours post-transfection. Accordingly, cells were washed with
507 1x PBS and collected in a microcentrifuge tube on ice. After centrifugation (4°C, 5 minutes,
508 200 rpm), cells were re-suspended with co-IP lysis buffer (25 mM Tris-HCl pH 7.4, 150 mM
509 NaCl, 10 mM EDTA, 1% NP-40, 5% glycerol) and supplemented with 1x EDTA-free protease

M1AP, ZZS & crossover formation

510 inhibitor cocktail (Roche, #11836170001). Samples were incubated for 15 minutes on ice and
511 collected by centrifugation (4°C, 15 minutes, 13000 rpm). The protein-containing supernatant
512 was transferred to a fresh microcentrifuge tube and directly processed or stored at –20°C until
513 further usage. When co-immunoprecipitation was conducted, a small amount of lysate was
514 kept for the ‘input’ protein validation.

515 **Co-immunoprecipitation**

516 Co-immunoprecipitation protocols were optimised and, depending on the respective protein-
517 protein interaction, two different types of magnetic beads were used for this study: Pierce™
518 magnetic anti-DYKDDDDK tag beads (Thermo Scientific, #A36797) for M1AP-SPO16 or anti-
519 HA tag beads (Thermo Scientific, #88838) for M1AP-SHOC1 as well as M1AP-TEX11. Beads
520 were equilibrated and pre-cleared according to the instructions and incubated with respective
521 protein lysates for 30 minutes at RT under gentle rotation. Anti-DYKDDDDK beads were
522 washed with 1x PBS three times; anti-HA beads were washed with 0.025% TBS-Tween six
523 times, and both were washed with double distilled water once. Gentle elution was achieved by
524 incubation with a Pierce™ 3x DYKDDDDK peptide (Thermo Scientific, #A36806) at 1.5 mg/ml
525 in 1x PBS for 5 minutes shaking or by using the Pierce™ elution buffer (pH 2, Thermo
526 Scientific, #21028) for 8 minutes. Beads were collected with a magnetic stand and
527 supernatants contained the eluted targets. Co-IP runs with pure bait lysates served as negative
528 controls. Samples were either stored at –20°C or processed directly.

529 **Western blotting**

530 Protein samples of either co-transfected DYK-M1AP, HA-SHOC1, HA-TEX11, or HA-SPO16,
531 ‘input’ samples of co-IP eluates, or singularly transfected bait IP controls were pre-mixed 1:4
532 with 4x Laemmli sample buffer (Bio-Rad, #1610747) supplemented with DTT (Merck,
533 #10197777001) and incubated at 95°C, 10 minutes for denaturation. Protein separation was
534 achieved using 4–15% mini-PROTEAN® TGX Stain-Free™ precast gels (Bio-Rad, #4568085)
535 for SDS polyacrylamide gel electrophoresis (SDS-PAGE). Proteins were transferred to a PVDF
536 membrane using the Trans-Blot® Turbo™ mini PVDF transfer packs (Bio-Rad, #1704156EDU)

M1AP, ZZS & crossover formation

537 following the manufacturer's instructions. Subsequently, membranes were blocked with 5%
538 milk powder solution in 0.025% TBS-Tween for 30 minutes at room temperature (RT).
539 Incubation of primary antibody diluted in blocking solution was performed overnight at 4°C.
540 Antibody details are listed in Appendix Table S3. Between the incubation steps, washing with
541 0.1% TBS-Tween was included. Peroxidase-conjugated secondary antibody incubation
542 followed. Visualisation was achieved by a chemiluminescence reaction using the Clarity™
543 Western ECL substrate kit (Bio-Rad, #1705060S) and the ChemiDoc MP imaging system (Bio-
544 Rad, #12003154). The molecular weights of analysed proteins were calculated using a
545 PageRuler™ plus prestained protein ladder (Thermo Scientific, #26619) and image procession
546 was performed using the Bio-Rad image lab software and molecular weight analysis tool (Bio-
547 Rad, #12012931). Samples shown in one figure were derived from the same experiment.

548 **Histological evaluation of testicular biopsies**

549 Testis biopsies of men with variants in *M1AP* or one of the ZZS genes and of control subjects
550 were obtained from testicular sperm extraction (TESE) approaches or histological
551 examinations at the Department of Clinical and Surgical Andrology of the CeRA, Münster, or
552 at the Clinic for Urology, Gießen, and were included for in-depth histological phenotyping.
553 Tissue samples were either snap-frozen, cryo-preserved (Sperm-Freeze™, Ferti-Pro, #3080),
554 or fixed in Bouin's solution, paraformaldehyde (PFA), or GR fixative overnight. Fixed samples
555 were washed with 70% ethanol and embedded in paraffin for routine histological examination.
556 Tissues were sectioned at 5 µm and stained with Periodic acid-Schiff (PAS) or haematoxylin
557 and eosin (H&E) according to standard protocols. If no differences between biopsies were
558 observed, further analysis focused on one biopsy per case. In addition, the most advanced
559 germ cell type was quantified, representing the percentage of elongated spermatids (ES),
560 round spermatids (RS), spermatocytes (SPC), spermatogonia (SPG), Sertoli cell-only (SCO),
561 and hyalinised tubules (tubular shadows, TS) per section.

562 **Immunohistochemical staining of human testicular tissue sections**

563 For immunohistochemistry (IHC), biopsy samples were sectioned at 3 µm and incubated in
564 Neo-Clear™ (Sigma-Aldrich, #109843) for de-paraffinisation. Re-hydration was performed in
565 a descending ethanol row (99%, 98%, 80%, and 70% EtOH, respectively). Between individual
566 incubation steps, washing was performed using Tris-buffered saline (1x TBS). Incubation and
567 washing steps were performed at RT, if not stated otherwise. Heat-induced antigen retrieval
568 followed at 90°C, using either sodium citrate buffer (pH 6, Thermo Scientific, #005000) or Tris-
569 EDTA buffer (pH 9, Zytomed Systems, #ZYT-ZUC029), depending on the respective
570 antibodies' specifications. Blocking of endogenous peroxidase activity and unspecific antibody
571 binding was achieved by incubation in 3% hydrogen peroxidase (H₂O₂, Pharmacy of the
572 University Hospital Münster, #1002187) for 15 minutes and in 25% normal goat serum (abcam,
573 #ab7481) diluted in TBS containing 0.5% bovine serum albumin (BSA, Merck, #A9647) for
574 30 minutes. Primary antibodies were diluted in 5% BSA-TBS and incubated in a humid
575 chamber at 4°C overnight, if not stated otherwise (for antibody details see Appendix Table S3).
576 Round spermatid arrest was scrutinised by cAMP responsive element modulator (CREM)
577 expression. Apoptosis of germ cells was analysed by TUNEL assay, following the
578 manufacturer's instructions (Thermo Scientific, #C10625). The progression of meiosis I was
579 evaluated by phospho-histone H2A.X (γH2AX) staining. Metaphase cells were detected by
580 phosphorylation of serine 10 on histone H3 (H3S10p). Incubation with unspecific
581 immunoglobulin G (IgG) adapted to the primary antibody host system or omission of the first
582 antibody (OC) served as negative controls (Appendix Figure S15). A secondary, biotinylated
583 goat anti-rabbit (abcam, #ab6012) or goat anti-mouse antibody (abcam, #ab5886) was
584 incubated for one hour, followed by conjugation with streptavidin–horseradish peroxidase
585 (HRP, Sigma-Aldrich, #S5512) for 45 minutes. Peroxidase activity was visualised by 3,3'-
586 diaminobenzidine tetrahydrochloride (DAB, Sigma-Aldrich, #D5905) incubation for 1–
587 20 minutes according to evaluation by microscope. The reaction was stopped in double
588 distilled water. Counterstaining was performed with Mayer's haematoxylin (Sigma-Aldrich,
589 #1092491000). De-hydration followed using increasing EtOH concentrations and finally, slides

590 were cleared with Neo-Clear™ and mounted with glass coverslips using M-GLAS® liquid cover
591 glass medium (Merck, #1.03973).

592 **Meiotic spermatocyte spreading**

593 Analysis of the effects of LoF variants in *M1AP*, *SHOC1*, *TEX11*, and *SPO16* on meiosis was
594 assessed on a single-cell level by meiotic spermatocyte spreading and subsequent
595 immunofluorescence staining. For this, snap-frozen or cryo-preserved (Sperm-Freeze™, Ferti-
596 Pro, #3080) testis samples were used (N=1 per gene [*M1AP*: M864, *SHOC1*: M2046, *TEX11*:
597 M3409, *SPO16*: M3863]). Processing was executed at RT if not stated otherwise. All solutions
598 were filtrated using a 0.2 µm filter. Samples were handled in 1x Dulbecco's phosphate-buffered
599 saline (D-PBS, Sigma-Aldrich, #14190) supplemented with 1.1 mM CaCl₂, 0.52 mM MgCl₂,
600 and sodium DL-lactate solution (D-PBS⁺). Seminiferous tubules were mechanically dissected
601 using two forceps and collected in 5 ml D-PBS⁺. Tubular remnants were allowed to settle for
602 5 minutes and supernatant was collected in a fresh tube. Centrifugation was performed for
603 5 minutes at 1000 rpm twice. The supernatant was discarded and the cell/nuclei pellet was re-
604 suspended in D-PBS⁺ to reach 15x10⁶ cells per ml. Of this, 10 µl were mixed with 20 µl 100 mM
605 sucrose (Thermo Scientific, #10134050) and dribbled on slides previously cleaned and dipped
606 in freshly prepared 1% PFA (Merck, #158127, pH 9.2 set with 10 mM sodium borate, Roth,
607 #8643) solution containing 0.15% Triton X-100 for fixation. Drying was performed for
608 90 minutes in a humid chamber with a closed lid and for another 45 minutes with the lid
609 opened. Slides were washed with 0.08% Photo-Flo (Kodak, #K1464510) solution for
610 10 seconds and dried completely. Either, immunofluorescence staining was performed directly
611 or slides were stored at -80°C until further processing followed.

612 **Immunofluorescence staining on spermatocyte spreads**

613 Slides were defrosted for 15 minutes at RT and washed with 1x PBS three times. All solutions
614 were filtrated using a 0.2 µm filter. The staining was divided into two parts to avoid cross
615 reactions and minimise foci-like background. First, non-specific binding was reduced via
616 blocking with 5% glycine (Sigma-Aldrich, #G7126), 0.3% Triton-X (Sigma-Aldrich, #T8787),

M1AP, ZZS & crossover formation

617 and 0.01% sodium azide (NaN₃, Sigma-Aldrich, #S2002) in PBS containing 5% normal donkey
618 serum (Merck, #S30). Rabbit, mouse, and goat primary antibodies were diluted in 0.3% Triton-
619 X and 0.01% NaN₃-PBS-Tween and successively incubated overnight at 4°C, for 30 minutes
620 at RT, and 15 minutes at 37°C in a humid chamber. Subsequently, slides were washed five
621 times in PBS and antibodies were coupled with fluorophore-conjugated secondary antibodies
622 for three hours at RT. Additional blocking steps followed: first in blocking solution with 5%
623 normal donkey serum, second with 5% normal goat serum (both for 15 minutes at RT), and
624 third by using 50 µg/ml anti-human Fab fragments in PBS (JacksonImmuno Research, #109-
625 007-003) for 60 minutes at RT in a humid chamber. Next, a second primary antibody incubation
626 was performed using human anti-centromere antisera (ACA, antibodiesinc, #15-234) and
627 coupled with an anti-human fluorophore-conjugated secondary antibody for 30 minutes at RT
628 as well as for one hour at 37°C. Finally, slides were washed five times in PBS and mounted
629 with ROTI® mount FluorCare medium (Roth, #HP19.1). Antibody details are provided in
630 Appendix Table S3.

631 **Image acquisition, processing, and digital data generation**

632 Immunohistochemical staining was captured with an Olympus BX61VS microscope and the
633 corresponding scanner software VS-ASW-S6, the PreciPoint O8 scanning microscope system,
634 or a Leica DM750 microscope and the Leica ICC50 HD camera. Immunofluorescence staining
635 of meiotic spreads was completed with a Zeiss Elyra 7 microscope for specialised 3D structured
636 illumination (SIM²) and the Zeiss Zen black software. Suitable filter sets (DAPI / GFP / TXR /
637 Y5) were used to visualise fluorophore-based antibody staining.

638 Image processing was achieved with the open-source software Fiji by ImageJ (v2.3.0/1.54h).
639 For down-streaming processing of images, pictures were cropped to desired sizes to ensure a
640 representative understanding of the testicular architecture or to allow focussed visualisation of
641 specific details. Meiotic progression was analysed by γH2AX localisation, and all tubules of
642 one cross section of each case were characterised by their most advanced prophase I stage.
643 Quantification of staining was performed using the PreciPoint ViewPoint software and in-build

M1AP, ZZS & crossover formation

644 measurement and counting tools (v1.0.0.9628). CREM- or TUNEL-positive cells were counted
645 per round tubule per cross section and presented as average number of positive cells per
646 tubule. Tubules were considered round when the ratio between the two diameters was in the
647 range of 1-1.5. The minimum number of counted tubules per section was $N = 25$, the maximum
648 number was $N = 177$. Class I crossover events were quantified for pachytene spermatocytes
649 spreads (only possible for control and M1AP), by counting the MLH1 foci per one
650 spermatocyte. Proper chromosome preservation was confirmed by ACA staining. Prophase I
651 stages were confirmed by SYCP1 or γ H2AX staining, depending on the respective co-labelling.
652 Given the limited amount of material, a minimum of ten pachytene spermatocytes were
653 analysed per case.

654 **Statistical analysis**

655 Data are presented as the mean with standard deviation (SD) for scatter plots or as mean with
656 range for bar graphs. Two-tailed Student's unpaired t-test was applied for all statistical
657 analyses using the GraphPad Prism software (v10.1.2). The difference was considered
658 significant when the P value was < 0.05 .

659 **Data availability**

660 Sequencing data of the MERGE study is available by contacting the Institute of Reproductive
661 Genetics (<https://reprogenetik.de>). Access to this data is limited for each case and specific
662 consent of the respective samples. All novel variants have been submitted to ClinVar
663 (SCV004708228 - SCV004708242).

664 **Acknowledgements**

665 We kindly thank all probands and their families for providing data, samples, and their contents
666 which are the foundation of our interdisciplinary biomedical research. Thomas Zobel and the
667 team from the [Multiscale Imaging Centre](#), University of Münster is thanked for his excellent
668 and professional support in SR-SIM microscopy (Elyra Zeiss Programmnummer INST
669 211/901-1 FUGB). The authors thank Celeste Brennecka for language editing. In addition, we
670 thank the following people for their valuable and professional support: Pascal Hauser, Lena

M1AP, ZZS & crossover formation

671 Schilling, Luisa Meier, Christina Burhöj, Alexandra Hax, Jochen Wistuba, Reinhild Sandhowe,
672 Willy Baarends, Lieke Koordneef, Esther Sleddens, Antoine Peters, Rita Exeler, Katja
673 Poorthuis, Adelheid Kerseboom, Elke Kößer, Sophie Koser, Claudia Krallmann, and Margot
674 Wyrwoll.

675 **Funding**

676 This study was carried out within the frame of the German Research Foundation-funded
677 Clinical Research Unit 'Male Germ Cells' (DFG CRU326, project number 329621271) to CF,
678 FT, NN and the German Academic Exchange Service (DAAD) to FT and MOB (project ID
679 57511796).

680 **Conflict of interest**

681 The authors declared no conflict of interest.

682 **Author contributions**

683 All authors revised and approved the final version of the manuscript. NR and CF conceived
684 and designed the experiments and wrote the manuscript. NR, JD, MDR, JK, AKD, SBW
685 performed the experiments. NR, JD, SDP, CR analysed the data. VN provided the MAR data.
686 DF, AP, NN, HCS, KA, SK, FT performed the case recruiting as well as clinical and histological
687 evaluation. BS, MOB, FT, CF provided critical feedback and supported this work by shaping
688 research progress and final results.

689 **References**

- 690 Arango, N.A., Huang, T.T., Fujino, A., Pieretti-Vanmarcke, R., Donahoe, P.K., 2006.
691 Expression analysis and evolutionary conservation of the mouse germ cell-specific
692 D6Mm5e gene. *Dev. Dyn.* 235, 2613–2619.
- 693 Arango, N.A., Li, L., Dabir, D., Nicolau, F., Pieretti-Vanmarcke, R., Koehler, C., McCarrey, J.R.,
694 Lu, N., Donahoe, P.K., 2013. Meiosis I arrest abnormalities lead to severe
695 oligozoospermia in meiosis 1 arresting protein (M1ap)-deficient mice. *Biol. Reprod.* 88,
696 1–11.
- 697 Bolcun-Filas, E., Handel, M.A., 2018. Meiosis: The chromosomal foundation of reproduction.
698 *Biol. Reprod.* 99, 112–126.
- 699 Börner, G.V., Hochwagen, A., MacQueen, A.J., 2023. Meiosis in budding yeast. *Genetics* 225,
700 1–33.
- 701 Börner, G.V., Kleckner, N., Hunter, N., 2004. Crossover/noncrossover differentiation,
702 synaptonemal complex formation, and regulatory surveillance at the leptotene/zygotene
703 transition of meiosis. *Cell* 117, 29–45.
- 704 De Massy, B., 2013. Initiation of meiotic recombination: How and where? Conservation and
705 specificities among eukaryotes. *Annu. Rev. Genet.* 47, 563–599.
- 706 De Muyt, A., Pyatnitskaya, A., Andréani, J., Ranjha, L., Ramus, C., Laureau, R., Fernandez-
707 Vega, A., Holoch, D., Girard, E., Govin, J., Margueron, R., Couté, Y., Cejka, P., Guérois,
708 R., Borde, V., 2018. A meiotic XPF–ERCC1-like complex recognizes joint molecule
709 recombination intermediates to promote crossover formation. *Genes Dev.* 32, 283–296.
- 710 Di Persio, S., Tekath, T., Siebert-Kuss, L.M., Cremers, J.F., Wistuba, J., Li, X., Meyer zu
711 Hörste, G., Drexler, H.C.A., Wyrwoll, M.J., Tüttelmann, F., Dugas, M., Kliesch, S., Schlatt,
712 S., Laurentino, S., Neuhaus, N., 2021. Single-cell RNA-seq unravels alterations of the
713 human spermatogonial stem cell compartment in patients with impaired

M1AP, ZZS & crossover formation

- 714 spermatogenesis. *Cell Reports Med.* 2, 100395.
- 715 Dunce, J.M., Dunne, O.M., Ratcliff, M., Millán, C., Madgwick, S., Usón, I., Davies, O.R., 2018.
716 Structural basis of meiotic chromosome synapsis through SYCP1 self-assembly. *Nat.*
717 *Struct. Mol. Biol.* 25, 557–569.
- 718 Enguita-Marruedo, A., Sleddens-Linkels, E., Ooms, M., de Geus, V., Wilke, M., Blom, E.,
719 Dohle, G.R., Looijenga, L.H.J., van Cappellen, W., Baart, E.B., Baarends, W.M., 2019.
720 Meiotic arrest occurs most frequently at metaphase and is often incomplete in
721 azoospermic men. *Fertil. Steril.* 112, 1059-1070.e3.
- 722 Ferguson, K.A., Wong, E.C., Chow, V., Nigro, M., Ma, S., 2007. Abnormal meiotic
723 recombination in infertile men and its association with sperm aneuploidy. *Hum. Mol.*
724 *Genet.* 16, 2870–2879.
- 725 Fernandez-Capetillo, O., Mahadevaiah, S.K., Celeste, A., Romanienko, P.J., Camerini-Otero,
726 R.D., Bonner, W.M., Manova, K., Burgoyne, P., Nussenzweig, A., 2003. H2AX is required
727 for chromatin remodeling and inactivation of sex chromosomes in male mouse meiosis.
728 *Dev. Cell* 4, 497–508.
- 729 Gray, S., Cohen, P.E., 2016. Control of Meiotic Crossovers: From Double-Strand Break
730 Formation to Designation. *Annu. Rev. Genet.* 50, 175–210.
- 731 Guiraldelli, M.F., Felberg, A., Almeida, L.P., Parikh, A., de Castro, R.O., Pezza, R.J., 2018.
732 SHOC1 is a ERCC4-(HhH)2-like protein, integral to the formation of crossover
733 recombination intermediates during mammalian meiosis. *PLoS Genet.* 14, e1007381.
- 734 Hamer, G., Roepers-Gajadien, H.L., Van Duyn-Goedhart, A., Gademan, I.S., Kal, H.B., Van
735 Buul, P.P.W., De Rooij, D.G., 2003. DNA double-strand breaks and γ -H2AX signaling in
736 the testis. *Biol. Reprod.* 68, 628–634.
- 737 Hassold, T., Hunt, P., 2001. To err (meiotically) is human: The genesis of human aneuploidy.

M1AP, ZZS & crossover formation

- 738 Nat. Rev. Genet. 2, 280-291.
- 739 Ioannou, D., Fortun, J., Tempest, H.G., 2019. Meiotic nondisjunction and sperm aneuploidy in
740 humans. *Reproduction*. 157:R15-R31.
- 741 Jan, S.Z., Jongejan, A., Korver, C.M., van Daalen, S.K.M., van Pelt, A.M.M., Repping, S.,
742 Hamer, G., 2018. Distinct prophase arrest mechanisms in human male meiosis. *Dev*. 145,
743 dev160614.
- 744 Kahraman, S., Sahin, Y., Yelke, H., Kumtepe, Y., Tufekci, M.A., Yapan, C.C., Yesil, M.,
745 Cetinkaya, M., 2020. High rates of aneuploidy, mosaicism and abnormal morphokinetic
746 development in cases with low sperm concentration. *J. Assist. Reprod. Genet.* 37, 629–
747 640.
- 748 Ke, H., Tang, S., Guo, T., Hou, D., Jiao, X., Li, S., Luo, W., Xu, B., Zhao, S., Li, G., Zhang, X.,
749 Xu, S., Wang, L., Wu, Y., Wang, J., Zhang, F., Qin, Y., Jin, L., Chen, Z.J., 2023.
750 Landscape of pathogenic mutations in premature ovarian insufficiency. *Nat. Med.* 29,
751 483–492.
- 752 Khan, M.R., Akbari, A., Nicholas, T.J., Castillo-Madeen, H., Ajmal, M., Haq, T.U., Laan, M.,
753 Quinlan, A.R., Ahuja, J.S., Shah, A.A., Conrad, D.F., 2023. Genome sequencing of
754 Pakistani families with male infertility identifies deleterious genotypes in SPAG6, CCDC9,
755 TKTL1, TUBA3C, and M1AP. *Andrology* 1–12.
- 756 Krausz, C., Riera-Escamilla, A., Moreno-Mendoza, D., Holleman, K., Cioppi, F., Algaba, F.,
757 Pybus, M., Friedrich, C., Wyrwoll, M.J., Casamonti, E., Pietroforte, S., Nagirnaja, L.,
758 Lopes, A.M., Kliesch, S., Pilatz, A., Carrell, D.T., Conrad, D.F., Ars, E., Ruiz-Castañé, E.,
759 Aston, K.I., Baarends, W.M., Tüttelmann, F., 2020. Genetic dissection of spermatogenic
760 arrest through exome analysis: clinical implications for the management of azoospermic
761 men. *Genet. Med.* 22, 1956–1966.
- 762 Lane, S., Kauppi, L., 2019. Meiotic spindle assembly checkpoint and aneuploidy in males

- 763 versus females. *Cell. Mol. Life Sci.* 76, 1135-1150.
- 764 Li, Y., Wu, Y., Khan, I., Zhou, J., Lu, Y., Ye, J., Liu, J., Xie, X., Hu, C., Jiang, H., Fan, S., Zhang,
765 H., Zhang, Y., Jiang, X., Xu, B., Ma, H., Shi, Q., 2023. M1AP interacts with the mammalian
766 ZZS complex and promotes male meiotic recombination. *EMBO Rep.* 24, e55778.
- 767 Macaisne, N., Novatchkova, M., Peirera, L., Vezon, D., Jolivet, S., Froger, N., Chelysheva, L.,
768 Grelon, M., Mercier, R., 2008. SHOC1, an XPF Endonuclease-Related Protein, Is
769 Essential for the Formation of Class I Meiotic Crossovers. *Curr. Biol.* 18, 1432–1437.
- 770 Nagirnaja, L., Lopes, A.M., Charng, W.L., Miller, B., Stakaitis, R., Golubickaite, I., Stendahl,
771 A., Luan, T., Friedrich, C., Mahyari, E., Fadiel, E., Kasak, L., Vigh-Conrad, K., Oud, M.S.,
772 Xavier, M.J., Cheers, S.R., James, E.R., Guo, J., Jenkins, T.G., Riera-Escamilla, A.,
773 Barros, A., Carvalho, F., Fernandes, S., Gonçalves, J., Gurnett, C.A., Jørgensen, N.,
774 Jezek, D., Jungheim, E.S., Kliesch, S., McLachlan, R.I., Omurtag, K.R., Pilatz, A.,
775 Sandlow, J.I., Smith, J., Eisenberg, M.L., Hotaling, J.M., Jarvi, K.A., Punab, M., Rajpert-
776 De Meyts, E., Carrell, D.T., Krausz, C., Laan, M., O'Bryan, M.K., Schlegel, P.N.,
777 Tüttelmann, F., Veltman, J.A., Almstrup, K., Aston, K.I., Conrad, D.F., 2022. Diverse
778 monogenic subforms of human spermatogenic failure. *Nat. Commun.* 13, 7953.
- 779 Nieschlag, E., Behre, H.M., Nieschlag, S., Kliesch, S., 2023. *Andrology*, 4th ed. Springer Berlin
780 Heidelberg, Berlin, Heidelberg.
- 781 Petit, F.M., Frydman, N., Benkhalifa, M., Le Du, A., Aboura, A., Fanchin, R., Frydman, R.,
782 Tachdjian, G., 2005. Could Sperm Aneuploidy Rate Determination Be Used as a
783 Predictive Test Before Intracytoplasmic Sperm Injection? *J. Androl.* 26, 235–241.
- 784 Pyatnitskaya, A., Borde, V., De Muyt, A., 2019. Crossing and zipping: molecular duties of the
785 ZMM proteins in meiosis. *Chromosoma*.128, 181-198.
- 786 Qi, Y., Wang, Y., Li, W., Zhuang, S., Li, S., Xu, K., Qin, Y., Guo, T., 2023. Pathogenic bi-allelic
787 variants of meiotic ZMM complex gene SPO16 in premature ovarian insufficiency. *Clin.*

M1AP, ZZS & crossover formation

- 788 Genet. 104, 486–490.
- 789 Rodrigo, L., Meseguer, M., Mateu, E., Mercader, A., Peinado, V., Bori, L., Campos-Galindo, I.,
790 Milán, M., García-Herrero, S., Simón, C., Rubio, C., 2019. Sperm chromosomal
791 abnormalities and their contribution to human embryo aneuploidy. *Biol. Reprod.* 101,
792 1091–1101.
- 793 Saraste, A., Pulkki, K., 2000. Morphologic and biochemical hallmarks of apoptosis.
794 *Cardiovasc. Res.*45, 528-537.
- 795 Song, N., Liu, J., An, S., Nishino, T., Hishikawa, Y., Koji, T., 2011. Immunohistochemical
796 analysis of histone H3 modifications in germ cells during mouse spermatogenesis. *Acta*
797 *Histochem. Cytochem.* 44, 183–190.
- 798 Sun, F., Mikhaail-Philips, M., Oliver-Bonet, M., Ko, E., Rademaker, A., Turek, P., Martin, R.H.,
799 2008. The relationship between meiotic recombination in human spermatocytes and
800 aneuploidy in sperm. *Hum. Reprod.* 23, 1691–1697.
- 801 Sun, F., Trpkov, K., Rademaker, A., Ko, E., Martin, R.H., 2005. Variation in meiotic
802 recombination frequencies among human males. *Hum. Genet.* 116, 172–178.
- 803 Tu, C., Wang, Y., Nie, H., Meng, L., Wang, W., Li, Y., Li, D., Zhang, H., Lu, G., Lin, G., Tan,
804 Y.Q., Du, J., 2020. An M1AP homozygous splice-site mutation associated with severe
805 oligozoospermia in a consanguineous family. *Clin. Genet.* 97, 741–746.
- 806 Vander Borght, M., Wyns, C., 2018. Fertility and infertility: Definition and epidemiology. *Clin.*
807 *Biochem.*62, 2-10.
- 808 Wang, S., Zickler, D., Kleckner, N., Zhang, L., 2015. Meiotic crossover patterns: Obligatory
809 crossover, interference and homeostasis in a single process. *Cell Cycle* 14, 305–314.
- 810 Weinbauer, G.F., Behr, R., Bergmann, M., Nieschlag, E., 1998. Testicular cAMP responsive
811 element modulator (CREM) protein is expressed in round spermatids but is absent or

M1AP, ZZS & crossover formation

- 812 reduced in men with round spermatid maturation arrest. *Mol. Hum. Reprod.* 4, 9–15.
- 813 World Health Organization, 2023. Infertility prevalence estimates, 1990-2021. Geneva.
- 814 Wyrwoll, M.J., Köckerling, N., Vockel, M., Dicke, A.K., Rotte, N., Pohl, E., Emich, J., Wöste,
815 M., Ruckert, C., Wabschke, R., Seggewiss, J., Ledig, S., Tewes, A.C., Stratis, Y.,
816 Cremers, J.F., Wistuba, J., Krallmann, C., Kliesch, S., Röpke, A., Stallmeyer, B.,
817 Friedrich, C., Tüttelmann, F., 2023a. Genetic Architecture of Azoospermia—Time to
818 Advance the Standard of Care. *Eur. Urol.* 83, 452–462.
- 819 Wyrwoll, M.J., Temel, Ş.G., Nagirnaja, L., Oud, M.S., Lopes, A.M., van der Heijden, G.W.,
820 Heald, J.S., Rotte, N., Wistuba, J., Wöste, M., Ledig, S., Krenz, H., Smits, R.M., Carvalho,
821 F., Gonçalves, J., Fietz, D., Türkgenç, B., Ergören, M.C., Çetinkaya, M., Başar, M.,
822 Kahraman, S., McEleny, K., Xavier, M.J., Turner, H., Pilatz, A., Röpke, A., Dugas, M.,
823 Kliesch, S., Neuhaus, N., Aston, K.I., Conrad, D.F., Veltman, J.A., Friedrich, C.,
824 Tüttelmann, F., 2020. Bi-allelic Mutations in M1AP Are a Frequent Cause of Meiotic Arrest
825 and Severely Impaired Spermatogenesis Leading to Male Infertility. *Am. J. Hum. Genet.*
826 107, 342–351.
- 827 Wyrwoll, M.J., van der Heijden, G.W., Krausz, C., Aston, K.I., Kliesch, S., McLachlan, R.,
828 Ramos, L., Conrad, D.F., O’Bryan, M.K., Veltman, J.A., Tüttelmann, F., 2023b. Improved
829 phenotypic classification of male infertility to promote discovery of genetic causes. *Nat.*
830 *Rev. Urol.* 21, 91-101.
- 831 Xie, C., Wang, W., Tu, C., Meng, L., Lu, G., Lin, G., Lu, L.Y., Tan, Y.Q., 2022. Meiotic
832 recombination: insights into its mechanisms and its role in human reproduction with a
833 special focus on non-obstructive azoospermia. *Hum. Reprod. Update* 28, 763–797.
- 834 Xu, R., Ding, Y., Wang, Y., He, Y., Sun, Y., Lu, Y., Yao, N., 2021. Comparison of
835 preimplantation genetic testing for aneuploidy versus intracytoplasmic sperm injection in
836 severe male infertility. *Andrologia* 53, e14065.

M1AP, ZZS & crossover formation

- 837 Yang, F., Gell, K., Van Der Heijden, G.W., Eckardt, S., Leu, N.A., Page, D.C., Benavente, R.,
838 Her, C., Höög, C., McLaughlin, K.J., Wang, P.J., 2008. Meiotic failure in male mice lacking
839 an X-linked factor. *Genes Dev.* 22, 682–691.
- 840 Yang, F., Silber, S., Leu, N.A., Oates, R.D., Marszalek, J.D., Skaletsky, H., Brown, L.G.,
841 Rozen, S., Page, D.C., Wang, P.J., 2015. TEX11 is mutated in infertile men with
842 azoospermia and regulates genome-wide recombination rates in mouse. *EMBO Mol.*
843 *Med.* 7, 1198–1210.
- 844 Yatsenko, A.N., Georgiadis, A.P., Röpke, A., Berman, A.J., Jaffe, T., Olszewska, M.,
845 Westernströer, B., Sanfilippo, J., Kurpisz, M., Rajkovic, A., Yatsenko, S.A., Kliesch, S.,
846 Schlatt, S., Tüttelmann, F., 2015. X-Linked TEX11 Mutations, Meiotic Arrest, and
847 Azoospermia in Infertile Men. *N. Engl. J. Med.* 372, 2097–2107.
- 848 Yu, X.C., Li, M.J., Cai, F.F., Yang, S.J., Liu, H. Bin, Zhang, H.B., 2021. A new TEX11 mutation
849 causes azoospermia and testicular meiotic arrest. *Asian J. Androl.* 23, 510–515.
- 850 Yuan, L., Liu, J.G., Zhao, J., Brundell, E., Daneholt, B., Höög, C., 2000. The murine SCP3
851 gene is required for synaptonemal complex assembly, chromosome synapsis, and male
852 fertility. *Mol. Cell* 5, 73–83.
- 853 Zhang, Q., Ji, S.Y., Busayavalasa, K., Yu, C., 2019. SPO16 binds SHOC1 to promote
854 homologous recombination and crossing-over in meiotic prophase I. *Sci. Adv.* 5,
855 eaau9780.
- 856 Zhang, Q., Shao, J., Fan, H.Y., Yu, C., 2018. Evolutionarily-conserved MZIP2 is essential for
857 crossover formation in mammalian meiosis. *Commun. Biol.* 1, 147.
- 858 Zickler, D., Kleckner, N., 2015. Recombination, pairing, and synapsis of homologs during
859 meiosis. *Cold Spring Harb. Perspect. Biol.* 7, 1–28.
- 860

Table 1. Genetic and testicular characteristics of infertile men with loss-of-function variants in *M1AP* or the *ZZS* genes

Case	Genetic variant (MAF gnomAD v4.1.0)	Semen analysis	Arrest type – most advanced germ cell type	TESE/MAR outcome	Reference
M1AP – autosomal-recessive inheritance, NM_138804.4					
M330		azoospermia	metaphase I arrest – elongated spermatids	negative	Wyrwoll et al., 2020
M864		azoospermia	metaphase I arrest – round spermatids	negative	Wyrwoll et al., 2020
M1792		azoospermia	NA	negative	Wyrwoll et al., 2020, Nagirnaja et al., 2022
M2062	c.[676dup];[676dup] p.[Trp226Leufs*4];[Trp226Leufs*4]	cryptozoospermia	metaphase I arrest – elongated spermatids	positive, ICSI failed	Wyrwoll et al., 2020, Wyrwoll et al., 2023
M2525	(MAF=0.003327)	azoospermia	metaphase I arrest – round spermatids	negative	
M2746		cryptozoospermia	metaphase I arrest – elongated spermatids	positive, ICSI successful	
M2747		cryptozoospermia	metaphase I arrest – elongated spermatids	negative	
M3402		azoospermia	metaphase I arrest – elongated spermatids	positive, ICSI failed	

M1AP, ZZS & crossover formation

M3511		azoospermia	metaphase I arrest – elongated spermatids	positive, ICSI failed	
M3609	c.[1073_1074+10del];[1073_1074+10del] p.[(Leu358Glnfs*58)];[(Leu358Glnfs*58)] (MAF=0.00006815)	azoospermia	metaphase I arrest – round spermatids	negative	
SHOC1 – autosomal-recessive inheritance, NM_173521.5					
M2012	c.[1085_1086del];[1085_1086del] p.[(Glu362Valfs*25)];[(Glu362Valfs*25)] (MAF: absent from gnomAD)	azoospermia	NA	NA	Krausz et al., 2020
G-377	c.[1085_1086del];[1085_1086del] p.[(Glu362Valfs*25)];[(Glu362Valfs*25)] (MAF: absent from gnomAD)	azoospermia	meiotic arrest – spermatocytes	negative	Nagirnaja et al., 2022
M2046	c.[1351del;1347T>A];[945_948del] p.[(Ser451Leufs*23;Cys449*);[Glu315Aspfs*6)] (MAF: absent; absent; 0.00001860)	azoospermia	meiotic arrest – spermatocytes	negative	Krausz et al., 2020
M3260	c.[1939+2T>C];[1939+2T>C] p.? (MAF: 0.000006309)	azoospermia	meiotic arrest – round spermatids	negative	

TEX11– X-linked inheritance, NM_001003811.2

M205	c.[1837+1G>C];[0] p.? (MAF: absent from gnomAD)	azoospermia	meiotic arrest – spermatocytes	negative	Yatsenko et al., 2015
M246	c.[22del];[0] p.(Ser8Profs*31) (MAF: absent from gnomAD)	azoospermia	meiotic arrest – spermatocytes	negative	
M281	c.[792+1G>A];[0] p.? (MAF: absent from gnomAD)	azoospermia	meiotic arrest – spermatocytes	negative	Yatsenko et al., 2015
M1390	c.[(204+1_205-1)_(737+1_738-1)del];[0] p.? (MAF: absent from gnomAD SVs v2.1)	azoospermia	meiotic arrest – spermatocytes	negative	Wyrwoll et al., 2023
M2739	c.[1052dup];[0] p.(Ser352Valfs*14) (MAF: absent from gnomAD)	azoospermia	meiotic arrest – NA	negative	
M2820	c.[(-157_-99+1)_(738-1_792+1)del];[0] p.? (MAF: absent from gnomAD SVs v2.1)	azoospermia	meiotic arrest – NA	negative	
M2942	c.[1245G>A];[0] p.(Trp415*) (MAF: absent from gnomAD)	azoospermia	NA	NA	
M3152	c.[(652-1_737+1)_(738-1_792+1)];[0] p.?	azoospermia	NA	NA	

M1AP, ZZS & crossover formation

(MAF: absent from gnomAD SVs v2.1)

M3409	c.[731G>A];[0] p.(Trp244*) (MAF: absent from gnomAD)	azoospermia	meiotic arrest – spermatocytes	negative
-------	--	-------------	-----------------------------------	----------

SPO16 – autosomal-recessive inheritance, NM_001012425.2

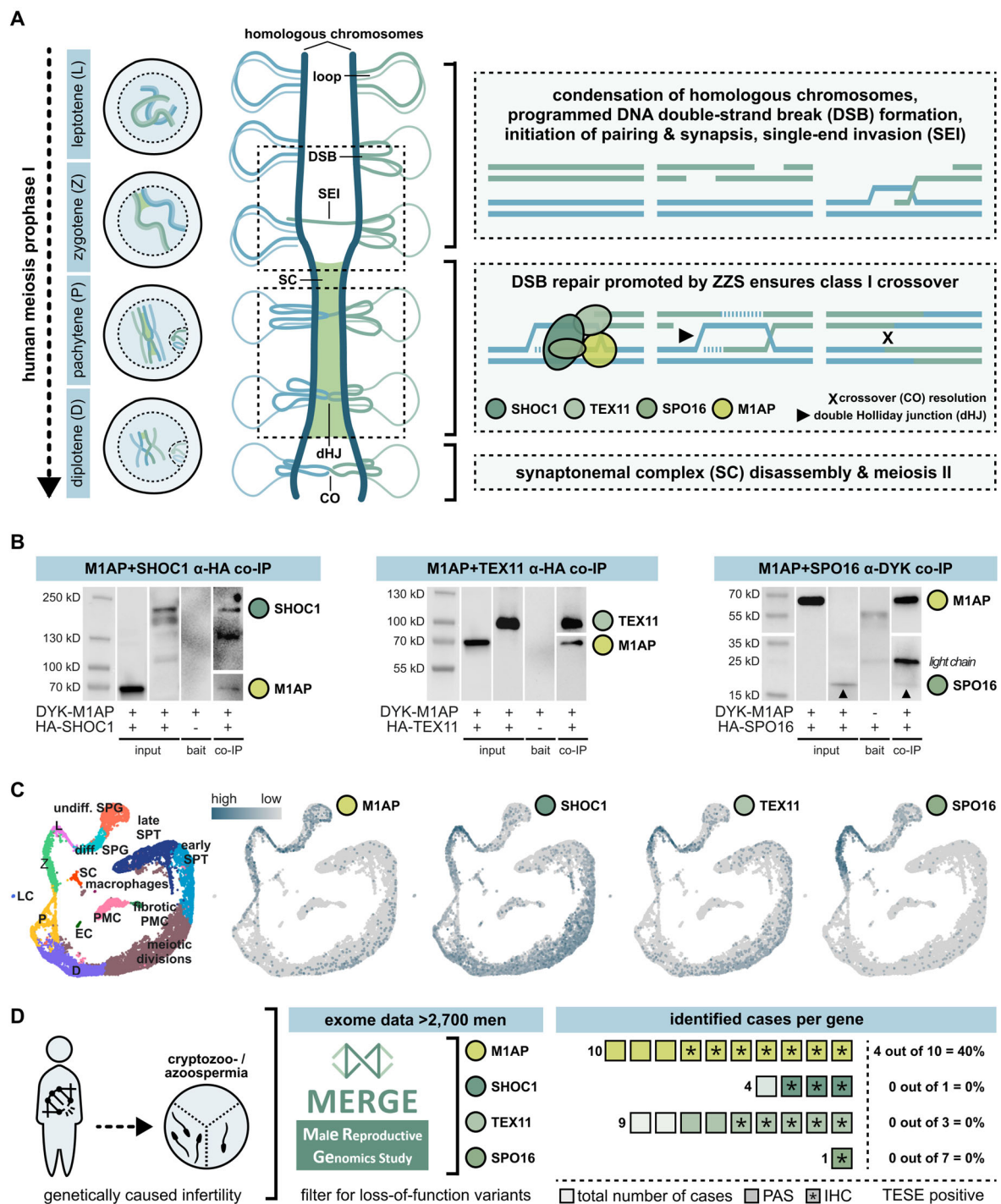
M3863	c.[266del];[266del] p.[(Leu89Trpfs*18)];[(Leu89Trpfs*18)] (MAF=0.000003724)	azoospermia	meiotic arrest – spermatocytes	negative
-------	---	-------------	-----------------------------------	----------

abbreviations: fs = frameshift, * = premature stop codon, NA = not available, TESE = testicular sperm extraction, MAR = medically assisted reproduction.

862

M1AP, ZZS & crossover formation

863 **Figures**



864

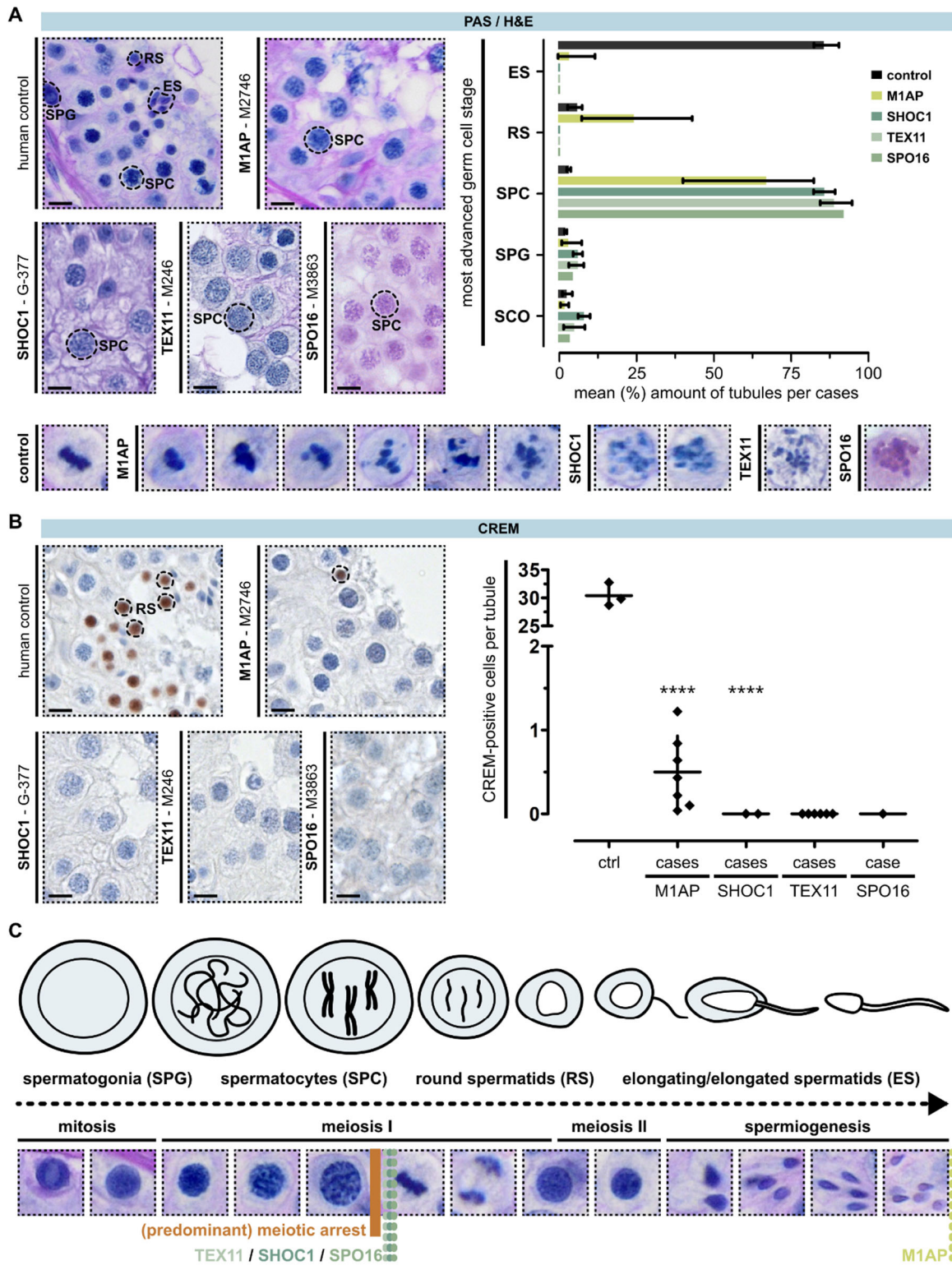
865 **Figure 1. Human meiotic recombination in men depends on ZZS function – and M1AP interacts with all**
 866 **three complex components.** A. Schematic representation of human prophase I and meiotic recombination. To
 867 simplify, the global arrangement of just one pair of homologous chromosomes is depicted and homologs are
 868 differentiated with two colours (blue, green). The molecular mechanisms of class I crossover resolution are
 869 represented in a simplified manner within the dotted boxes. In leptotene (L), homologous chromosomes
 870 condensate, and align. DNA double-strand breaks (DSBs) are initiated. During zygotene (Z), homologous
 871 chromosomes pair up and the initiation of synapsis is supported by the dynamic assembly of a ladder-like structure
 872 – the synaptonemal complex (SC). This complex provides structural basis for meiotic recombination and in
 873 pachytene (P), the chromosomes are fully synapsed. DSB repair results in at least one crossover (CO) per
 874 chromosome pair (= obligatory crossover principle) and highly depends on SHOC1, TEX11, and SPO16 (= ZZS
 875 complex) activity. An integration of M1AP in this process was shown in mice (Li et al., 2023). Cells have
 876 completed DSB repair in diplotene (D), the SC disassembles, and homologs are physically connected by
 877 chiasmata. B. Co-immunoprecipitation (IP) proved the interaction of human M1AP (detected by N-terminal
 DYK-tag) with each of the

M1AP, ZZS & crossover formation

878 ZZS complex proteins (detected by C-terminal HA-tag). Input and bait proteins served as positive and negative
879 controls. Respective co-IP Western blot panels can be read from left to right as following: 1st lane = marker, 2nd =
880 co-transfection of both plasmids, detection of M1AP in input sample, 3rd = co-transfection of both plasmids, detection
881 of ZZS in input sample, 4th = transfection of bait protein only and detection after co-IP (negative control), 5th = co-
882 transfection of both plasmids, detection of both proteins from co-IP sample. In the last panel, the upturned arrow
883 head indicates the faint bands of SPO16 for better visualisation. Due to the low detection signal of SPO16, antibody
884 chains of the co-IP specific anti-DYKDDDDK antibody, detected with anti-mouse HRP secondary antibody, are
885 visible too. C. Uniform manifold approximation and projection (UMAP) plot of obstructive azoospermic controls
886 (N=3) adapted from Di Persio et al., 2021. Through mRNA expression profiling, individual stages of human
887 spermatogenesis were clustered and visualised. Expression data of human *M1AP*, *SHOC1*, *TEX11*, and *SPO16*
888 mRNA was compiled by querying the dataset. D. For each gene, variants leading to dysfunctional proteins were
889 searched for in the MERGE study dataset to associate a deficient genotype with a distinct phenotype. Overall, ten
890 men with LoF variants in *M1AP*, four men with LoF variants in *SHOC1* (N=3 from MERGE and N=1 from GEMINI),
891 nine men with LoF variants in *TEX11*, and one man with a LoF variant in *SPO16* were selected. If possible, material
892 aiming for testicular sperm extraction (TESE) was used for subsequent analyses including periodic acid-Schiff
893 (PAS) or haematoxylin and eosin (H&E) staining (both highlighted in bolder colour), immunohistochemical staining
894 (IHC = *), and spermatocyte spreads (one sample per gene of interest). A positive TESE result was only seen in
895 men with LoF variants in *M1AP* (N=4).

896

M1AP, ZZS & crossover formation



897

898 **Figure 2. Testicular phenotyping of men with loss-of-function variants in *M1AP*, *SHOC1*, *TEX11*, and *SPO16*.**
 899 A. PAS staining of testicular tissue with full spermatogenesis and infertile men with LoF variants in genes encoding
 900 the ZZS proteins and M1AP. One representative case per gene is depicted (*M1AP*: M2746, *SHOC1*: G-377, *TEX11*:
 901 M246, *SPO16*: M3863). For all biopsies, the most advanced germ cell type per tubule was assessed and is shown
 902 in the representative image and the bar graph. In addition, intact (control, M1AP) metaphase and aberrant (M1AP,
 903 SHOC1, TEX11, SPO16) metaphase-like cells were observed (detail view). **** $p \leq 0.0001$ compared to controls.
 904 B. Haploid germ cells were analysed by CREM localisation. Only men with LoF variants in *M1AP* had CREM-
 905 positive round spermatids. Compared to the controls, the total amount of these cells was significantly reduced. C.
 906 Schematic illustration and corresponding PAS staining of human spermatogenesis. Coloured dotted lines represent
 907 the identified gene-specific germ cell arrest. SPG: spermatogonia, SPC: spermatocytes, RS: round spermatids, ES:
 908 elongated spermatids. The scale bar represents 10 μ m.

M1AP, ZZS & crossover formation

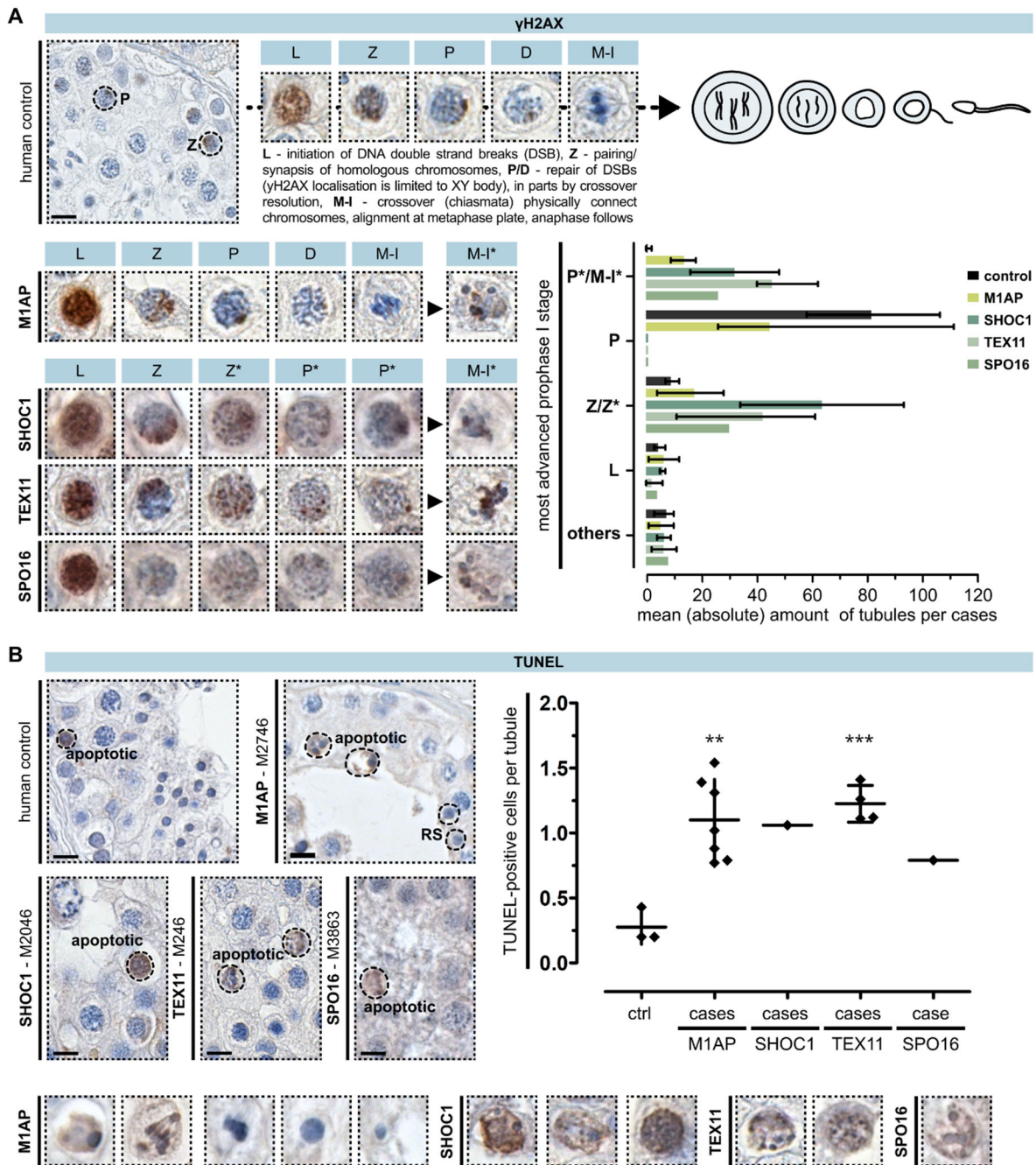
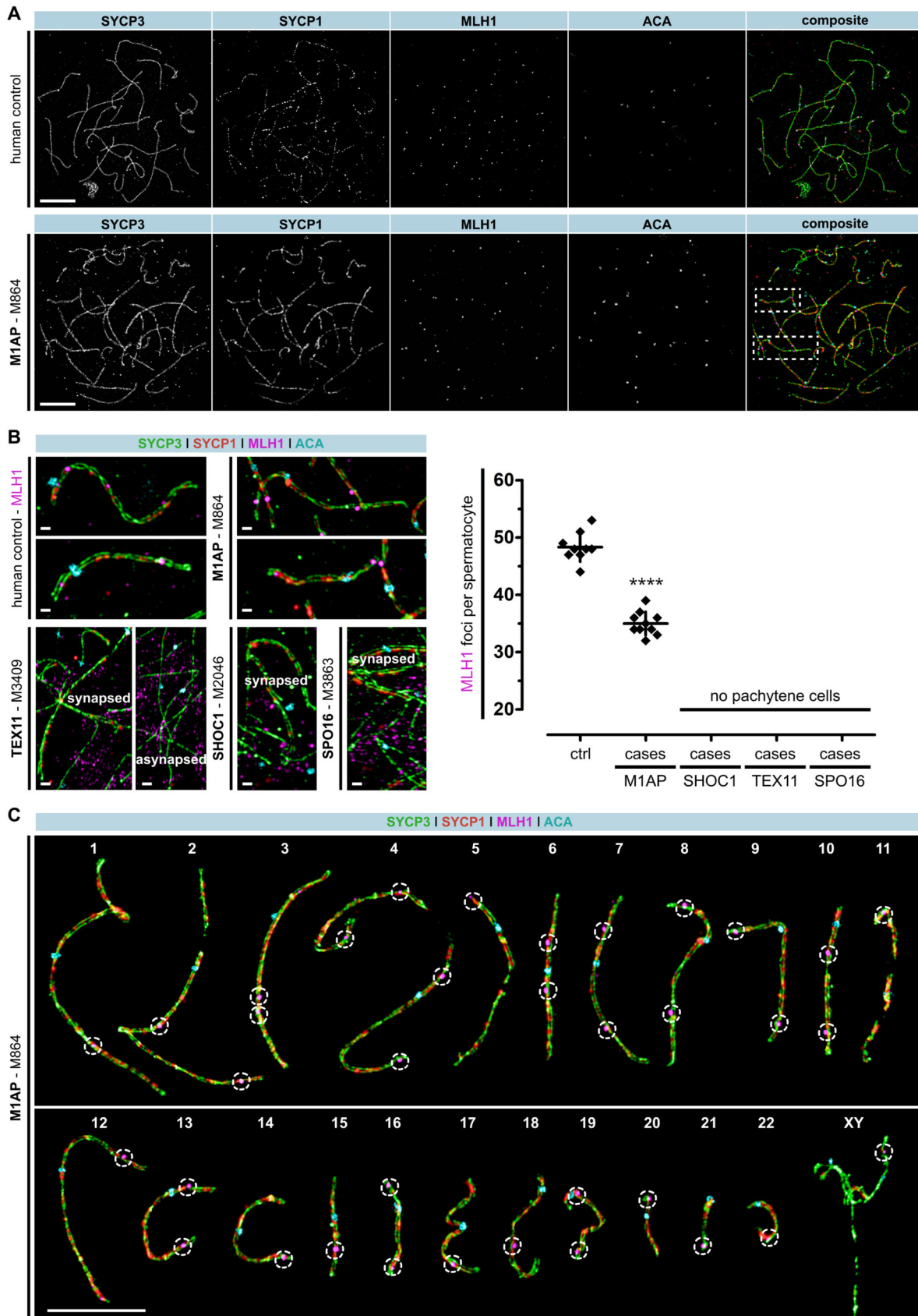


Figure 3. Investigation of meiotic recombination and arrest in men with loss-of-function variants in *M1AP*, *SHOC1*, *TEX11*, and *SPO16*. A. Localisation of yH2AX in a control demonstrates the marker's specific staining pattern during each substage of meiosis prophase I. Analysis of this marker in the infertile men revealed genotype-specific aberrations and meiotic arrest: M1AP = partial metaphase (M-I) arrest, SPO16/TEX11/SHOC1 = zygotene-(Z*) to early pachytene-like (P*) arrest, with occasional metaphase-like cells (M-I*). B. TUNEL assay showed increased apoptosis in patients independent of the genetic background (dot plot). Most TUNEL-positive cells already showed hallmarks of apoptosis (detail view), and only men with LoF variants in *M1AP* showed TUNEL-negative metaphase cells with correctly aligned chromosomes, round, and elongated spermatids. **p < 0.01, ***p < 0.001 compared to controls. The scale bar represents 10 μ m.

M1AP, ZZS & crossover formation



919

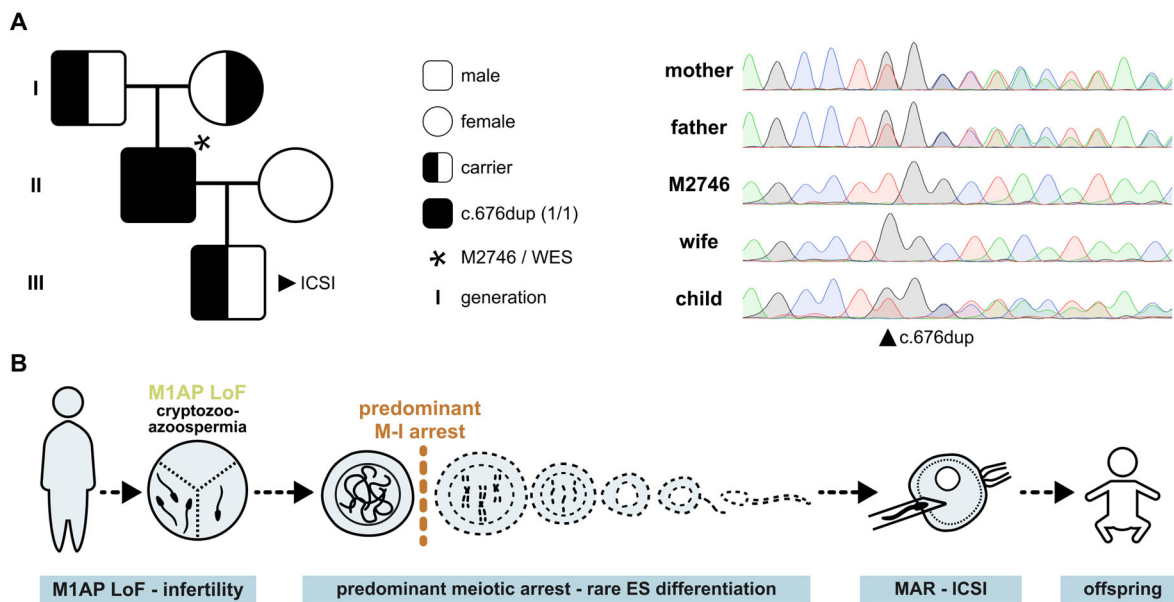
920
921
922
923
924
925

Figure 4. A man with loss-of-function variant in *M1AP* showed reduced MLH1 foci. A. Human spermatocyte spreads were stained for synaptonemal complex formation (= SYCP3, green + SYCP1, red), centromeric regions (= ACA, cyan), and designated crossover sites (= MLH1, magenta). A control and M864, deficient for M1AP, were compared. B. MLH1 localisation was seen on synapsed chromosome axes of pachytene-like spermatocytes in the control and M864. The total number of MLH1 foci per spermatocyte was reduced in M864. In contrast, men deficient for SHOC1 (M2046), TEX11 (M3409), or SPO16 (M8363) completely lacked pachytene-like cells. Instead,

M1AP, ZZS & crossover formation

926 spermatocytes showed increased asynapsed chromosomes where SYCP1 localisation was lacking. No MLH1 was
927 seen because cells arrested in a zygotene-like stage. **** $p \leq 0.0001$ compared to control. C. Super resolution
928 structured illumination microscopy (SR-SIM) of one spreaded spermatocyte. Homologous chromosomes were
929 digitally separated to mark the MLH1 foci (dotted circles), which represent the sites of class I crossover. In this
930 spermatocyte, each pair of homologues has at least one MLH1 focus and, thus, the *obligatory crossover* principle
931 is met. The scale bars represent 10 μm and 1 μm for magnification.

M1AP, ZZS & crossover formation



932

933

934

935

936

937

938

Figure 5. Proof-of-principle: M1AP-associated infertility can be overcome by medically assisted reproduction (MAR). A. One man (M2746) with a loss-of-function variant in *M1AP* was diagnosed with cryptozoospermia and predominant meiotic arrest. Three cycles of intracytoplasmic sperm injection (ICSI) with ejaculate-derived spermatozoa resulted in the birth of a healthy boy. Segregation analysis showed the autosomal-recessive inheritance pattern of the frameshift variant c.676dup. B. Illustration of how predominant meiotic arrest caused by M1AP-associated infertility still enables fatherhood.